Characterization of Flow Control Using Programmable Multi-Directional Plasma Actuators

by

Samuel W. Gustin

A thesis submitted to the
School of Graduate and Postdoctoral Studies in partial
fulfillment of the requirements for the degree of

Masters of Applied Science In Mechanical Engineering

Department of Mechanical and Manufacturing Engineering

University of Ontario Institute of Technology (Ontario Tech University)

Oshawa, Ontario, Canada

September 2023

THESIS EXAMINATION INFORMATION

Submitted by: **Samuel Gustin**

Masters of Applied Science in **Mechanical Engineering**

Thesis title: Characterization of Flow Control Using Programmable Multi-Directional Plasma Actuators

An oral defense of this thesis took place on August 17, 2023 in front of the following examining committee:

Examining Committee:

Chair of Examining Committee	
Research Supervisor	Dr. Martin Agelin-Chaab
Examining Committee Member	Dr. Horia Hangan
Thesis Examiner	Dr. Hossam Gaber, Professor Faculty of Engineering and Applied Science

The above committee determined that the thesis is acceptable in form and content and that a satisfactory knowledge of the field covered by the thesis was demonstrated by the candidate during an oral examination. A signed copy of the Certificate of Approval is available from the School of Graduate and Postdoctoral Studies.

ABSTRACT

This research explores the use of a novel plasma actuator geometry and electrical configuration to generate directionally programmable flow fields near the surface of arrays of such plasma actuators. Plasma actuators are unique ionothrusters which are reliant on geometry to define flow directionality. This thesis defines and makes use of a new class of plasma actuator which can generate directionally differentiated flows within a single geometry via use of high voltage switches and specialized geometries. The multi-directional plasma actuators are trialed individually and in arrays and the space defined by the directionality of flows which can be generated is defined. It is found that these devices are capable of generating flows sufficient to create flow modifications which are beneficial for the efficiency and control of lifting bodies and airframes. The research demonstrates that the described programmable, multi-directional, plasma actuators may be used to create an assortment of desired flows and to aid in the control of airframes.

Keywords: fluid dynamics; aircraft control; plasma actuators

AUTHOR'S DECLARATION

I hereby declare that this thesis consists of original work of which I have authored. This is a true copy of the thesis, including any required final revisions, as accepted by my examiners.

I authorize the University of Ontario Institute of Technology (Ontario Tech University) to lend this thesis to other institutions or individuals for the purpose of scholarly research. I further authorize University of Ontario Institute of Technology (Ontario Tech University) to reproduce this thesis by photocopying or by other means, in total or in part, at the request of other institutions or individuals for the purpose of scholarly research. I understand that my thesis will be made electronically available to the public.

Samuel Gustin

STATEMENT OF CONTRIBUTIONS

I hereby certify that I am the sole author of this thesis and that no part of this thesis has been published or submitted for publication. I have used standard referencing practices to acknowledge ideas, research techniques, or other materials that belong to others. Furthermore, I hereby certify that I am the sole source of the creative works and/or inventive knowledge described in this thesis.

ACKNOWLEDGEMENTS

Thank you to my wife Hilary who was my ever present supporter and sounding board during this work. Without her trust in me, I would never have been able to keep going and get this completed. Also thank you to Dr Agelin-Chaab whose wisdom, guidance, and eminently patient approach with me made it possible to complete this work. I do not think I could have done this with any other advisor.

TABLE OF CONTENTS

LIST OF TABLES

Chapter 3

LIST OF FIGURES

CHAPTER 2

CHAPTER 3

CHAPTER 4

LIST OF ABBREVIATIONS AND SYMBOLS

A	Saturation Ionization
B	Experimental constant from Paschen's Law
ArPEl	Array of Plasma Elements
C_D	Coefficient of Drag
C_L	Coefficient of Lift
d	Gap distance between exposed and encapsulated electrodes
DBD	Dielectric Barrier Discharge Plasma Actuator
DEE	Double Encapsulated Electrode (plasma actuator)
GPIO	General Purpose Input/Output
IGBT	Insulated Gate Bipolar Transistor
m	Number of the basis vector in question (range = [0,n)
MDBD	Multi Dielectric Barrier Discharge (plasma actuator)
n	Number of faces on the regular convex polynomial used as the exposed electrode
p	Pressure
PEl	Plasma Element, a multi-directional dielectric barrier discharge plasma actuator
PIV	Particle Image Velocimetry
MCU	Microcontroller Unit
RTC	Real Time Clock
SDBD	Single Dielectric Barrier Discharge (plasma actuator)
STP	Standard Temperature and Pressure (0^oC and 100kPa)
V_B	Breakdown voltage
φ	Angle of the m^{th} basis vector
θ	Angle between basis vectors
γ_{se}	Secondary electron emission coefficient

Chapter 1. Introduction

1.1 Background Analysis

Ionic wind propulsion is the concept of using a device called an ionic thruster, or ion thruster, to generate electrical plasmas and accelerate that plasma through an electrical potential, thereby generating thrust. The first observation of ionic wind was reported by Francis Hauksbee [1] in 1709 when he was experimenting with glow discharges generated by high voltage electricity. This research naturally led to the discovery of this effect as the goal of his glow-discharge research focused on generating high voltage electrical plasmas, and it is possible to generate this effect in earth's atmosphere at Standard Temperature and Pressure (STP) by creating a sufficiently intense voltage gradient across an air gap (~1Kv/mm) in the presence of an electromagnetic field. This voltage gradient strips electrons from the neutral atmosphere and generates an electrical plasma, which descends through the potential field producing thrust.

For several hundred years, this research into thrust generated via ionic wind was something of a scientific curiosity but found no applications in industry. It was not until the advent of heavier than air aircraft, and particularly once the limitations inherent in propeller driven craft had been reached, that this research was re-opened. In the 1960s, a United States military researcher performed research focusing on exploring the potential use of ion thrusters in aircraft applications [2]. During this period, there was a great deal of research, both scientific and pseudo-scientific, into the possibility of using ion thrusters as an alternative for jet or propellor aircraft thrust systems. Ultimately the scientific research showed that ion

thrusters were not sufficiently efficient to act as primary thrust devices for any reasonably sized aircraft. Meanwhile, scandals produced by high profile pseudo-scientific reports led to the field being considered non-credible for a number of decades.

The domain of research did not reopen materially until the late 1990s and early 2000s when a pair of papers, one by Corke et al. [3] and another by Roth et al. [4], focusing on the use of simplified ion thrusters to control boundary layer flows showed the promise of these simplified devices for boundary layer flow control. These simplified devices are called Plasma Actuators, and they are a form of ionic thruster where the ionizing element and the component that generates the electrical potential to accelerate the plasma are combined into one component.

The research by these groups showed the capacity for plasma actuators to modify boundary layer flows and possibly to optimize these plasma actuators to be effective as flow modification devices similar to other active flow control techniques. Specifically, they showed it was possible to modify the behavior of a lifting body by inducing flows in the boundary layer near the surface of a lifting body. This new vector of research into these devices has shown promise, with teams developing even more simplified forms of plasma actuators such as dielectric barrier discharge (DBD) plasma actuators and into the effects these can have on aircraft control.

1.2 Motivation

There is a desire in the aviation and wind energy industries to have low cost, low weight options for controlling the aerodynamic behavior of airframes. Over the past

twenty years, it has been established that plasma actuators are able to induce a variety of beneficial behaviors in lifting bodies, such as wings and turbine blades. One major barrier to the wider adoption of plasma actuators as airflow modifiers is that many desired behaviors require specific actuator geometries which are mutually exclusive between behaviors. That is to say, the position or electrode geometries required for one modification are not compatible with the geometry required to induce a different behavior. This research describes a regular array of plasma actuators capable of inducing flow in any direction near the surface of an array. This can then be used as the basis for inducing the desired behaviors anywhere on the array at any time.

1.3 Objectives

The central goal of this research is to develop principles required to implement large scale multi-directional plasma actuator arrays (ArPEls) by displaying full directional control over a small array. The specific objectives are:

- Develop an architecture for multi directional plasma actuators where direction of induced flow can be controlled without changing the physical characteristics of the device.
- Develop a regular array of multi directional plasma actuators capable of directional control.
- Implement and display full directional control over a small array in the plane of the array.
- Demonstrate flow control in three dimensions for flows near the surface of the Array of Plasma Elements (ArPEl).

In order to ensure that these proposed Multi Directional DBD Plasma Actuators (Plasma Elements for short) are able to produce any desired flow direction within the plane of the array, the geometry must meet certain requirements. When defining the axes of a plasma element, the average direction of the interface between the exposed and encapsulated electrodes is the primary factor in the directions in which momentum can be added to the flow. This interface is where the activation of the air takes place, and the induced momentum will be in a direction that is normal to this average line pointing towards the encapsulated electrode. As such, by considering the unit vectors originating on this average line, normal to the line, and pointing towards the encapsulated electrode, it is possible to define the primary axes of the plasma element. For a square plasma element such as that studied herein, these axes intersect at the center of the exposed electrode and point outwards in all four directions at 90^{o} to each other, similar to the axes of the cartesian plane.

Plasma elements operating under AC voltage only function in the direction of the encapsulated electrode. As such, the primary axes defined above are colinear to the primary directions in which momentum can be induced in such a device. If a device such as the one described is expected to produce arbitrary flow directions, it is necessary that these axes additively span the vector space of the plane of the expected flows. In order to reduce complexity, this research is restricted to plasma actuators which form a strict basis for the possible vectors within the plane of the array.

In order to demonstrate full flow control near the surface of an array, this work will make use of small arrays and Particle Image Velocimetry (PIV) systems to track and quantify the flow control demonstrated by the system. The goal of this work is to show control of the flow in arbitrary directions in the plane of the array and as angled jets out of the surface near the surface of the array. Specifically, it should demonstrate that an array comprising repeating elements of a single geometry is able to reproduce 5 desirable flow regimes which were previously mutually exclusive.

1.4 Scope

The first aspect of this research focuses on the physical geometry and materials required to create a directionally controllable plasma actuator. As this type of plasma actuator is novel in concept, this geometry must be revised through experimentation. The metrics for success of this stage are that the design be easily producible, tolerant of manufacturing error margins, and capable of producing flow from at least three directions so as to create a positive basis for the vector space of desired induced airflows in-plane with the array.

The second aspect aims to demonstrate that the device and software will provide functional control of flow in three dimensions near the surface of the array. Such control ensures the ability to generate flow capable of producing the desirable modifications to the properties of the body moving through the freestream flow. The metric for determining success will be to first establish that flow can be controlled along the principal axes of a single Multi-directional Plasma Element (PEl). Secondly, the flow must be controlled in the plane of the PEl and at an angle

to the principal axes. Lastly, flow out of the plane and at an angle to any major axis is demonstrated by making use of multiple PEls.

In order to establish this control, a PIV system is used to make three dimensional models of the flow induced above a firing PEl. These models show the induced flow attributes such as direction, velocity, and entrainment. These results allow for the quantitative measurement of the average flow rate and the direction within the test volume. Further, these results provide qualitative evidence of the effect on the entrained flows and the ability to control velocity along primary axes using the switching system.

Having established control over flow coaxial to the primary axes of the plasma elements, it is possible to repeat the process while tuning the system to use multiple encapsulated electrodes at varying duty cycles to induce off-axis flows. The same PIV approach can provide evidence to quantify the induced velocity within the test volume to establish the level of control over directionality as a function of varying duty cycles. This establishes full flow control within the plane and the ability to induce momentum in directions that are not colinear to any primary axis of any plasma element.

Now, with arbitrary flow control within the plane demonstrated, it remains to use multiple PEls arranged in a regular array to produce flows normal to the plane of the array and at angles out of the plane of the array. This will establish complete control over near-boundary flows and the ability to induce arbitrary flows.

Having established that a basic ArPEl is able to modify flow in any direction, it is reasonable to claim that these regular arrays will be able to replicate the results of prior experiments without specialized geometries. This forms the basis of a system with applications in flight control, blade efficiency management, and vibration control.

1.5 Thesis Structure

The rest of the thesis is structured as follows. Chapter 2 contains a comprehensive literature review on the historical and contemporary state of research into the use of dielectric plasma actuators for flow modification. Chapter 3 provides a detailed methodology outlining the experimental research undertaken to develop and demonstrate the efficacy of our PEl and ArPEl apparatus. Chapter 4 presents the results and discussion demonstrating that the experiments undertaken provide compelling evidence that general flow control near a surface can be achieved using ArPEls. Finally, Chapter 5 provides the concluding remarks as well as recommendations for future works.

Chapter 2. Literature Review

A brief review of the history of research leading to Dielectric Barrier Plasma Elements, the proposed uses for such apparatus throughout history, the physical and electrical requirements of such devices, and the modern state of the research into these devices. This section begins by describing the early research in which a combination of scientists and charlatans attempted to make high power DBD plasma actuators for use as solid-state engines for early aircraft. A hiatus in research occurred before seminal works in the nineties re-invigorated the field, and new, more scientifically rigorous research began into the subject. This section expands on a variety of research which has led to the identification of several flow modifications which can be used to modify the flight behaviour of aircraft.

Having identified that there are desirable effects which can be generated via DBD plasma actuators, the effects of these modifications, along with the requirements for inducing them, are outlined. The physical apparatus of DBD plasma actuators are outlined, and particular attention is paid to the geometry and construction of these devices. This highlights the construction requirements for such devices, along with the mutual incompatibility between differing geometries designed to generate differing flows.

With an understanding of the physical requirements of the devices, electrical requirements are outlined. These devices require high voltage alternating current or high voltage pulses to operate. The electrical impact on performance is outlined, and the electrical requirements for operation are described. These inform later discussions on electrical switching and control over apparatus.

Finally, having described the history and effects of DBD plasma actuators along with the electrical and physical requirements for their operation, gaps in the current state of research are outlined. The limitations caused by the physical principles which govern plasma generation in DBD plasma actuators and the entrainment above them are highlighted. Opportunities for trade-offs between physical and electrical complexity are described. Ultimately this section outlines the need for a device where flow directionality can be controlled through electrical systems within a single physical geometry is outlined.

2.1 History and Origins of Plasma Actuators

Plasma actuators themselves stem from a type of device called an ionocraft in which an electrical plasma is produced by electrically ionizing gas and then accelerating it over an electrical potential. Plasma actuators are a special type of ionocraft in which the ionizing and accelerating elements are combined into one phase, thus making them much simpler and more robust than other ionic thrusters. While similar devices were first invented over three hundred years ago [1], it was only in the early 1960s that research focused on plasma actuators as potential thrusting devices for electric aircraft explored [2]. While this effort ultimately failed to produce large ionocraft for military applications, it did lay the groundwork for much of the geometry and physical theory of how ionocraft works. However, this initial failure, coupled with high profile scandals of some pioneers of this concept [5] resulted in the neglect of the area and a focus on traditional aerodynamic and geometric flow controls, such as thrust-vectoring and active air vectoring.

The late 1990s and early 2000s saw some revival of plasma actuator research with a focus on active flow control. This was initiated by the seminal papers of Roth et al. (1998) [4] and Corke et al. (2002) [3], which pioneered the application of plasma actuators on airfoils. In these papers, the focus of plasma actuator research was shifted away from propulsion and toward flow control and boundary layer optimization. Both Roth and Corke's first papers focused primarily on a rudimentary exploration of the effects of different orientations of simple plasma actuators, and neither was able to produce improvements exceeding those possible by simple geometric changes to the wing itself.

Despite their limited scope and the wanting efficacy of their results, these papers provided the proof of concept for altering the aerodynamic properties of wings via the use of plasma actuators, which helped lead to a boom in plasma actuator research. In the decade and a half since these papers, a great deal of research has been done on the applications of plasma actuators to wings. Today this has led to three major overarching areas of research; the development of computer models of the effects of plasma actuators on flows, the design of plasma actuators, and research into the coupling of plasma actuators with the flow around them.

2.2 Operating Principles of Plasma Actuators

Simple dielectric barrier discharge plasma actuators such as the one shown in figure 2-1 all feature four common properties. 1. All DBD plasma actuators feature an exposed electrode capable of conducting high voltage current such as a metal foil. Copper is commonly chosen for this application. 2. All DBD plasma actuators feature at least one encapsulated electrode which is also conductive and

is commonly made from the same material as the exposed electrode. 3. DBDs feature a dielectric material used to separate the encapsulated and exposed electrodes. And 4. All DBDs are powered by some non-steady high voltage power supply. For this application AC current, pulsed current, and DC-offset AC are all acceptable options which optimize for different effects.

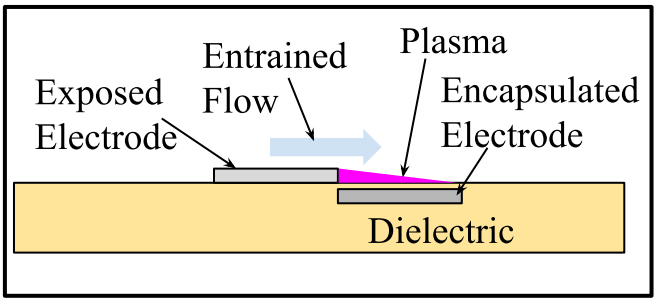

Figure 2-1A dielectric barrier discharge plasma actuator

The primary operating principle of dielectric barrier discharge plasma actuators is that cold plasma is formed along the edge of the exposed electrode and travels down potential through the electromagnetic field established by the potential difference across the exposed and encapsulated electrodes. In order for this plasma to form it is required that the electromagnetic field gradient be strong enough to ionize air at STP. The critical threshold for voltage required to ensure this ionization occurs is closely modeled, for small gaps between the encapsulated and exposed electrodes, by Paschen's Law as shown in equation.

Equation 2-1 Paschen's Law

$$V_B = \frac{Bpd}{\ln(Apd) - \ln\left(\ln 1 + \frac{1}{\gamma_{se}}\right)}$$

2.2 Effects of Plasma Actuators on Airflows

The most critical element in the development of an array such as the one proposed is an understanding of the effects that plasma actuators have on the flow over airfoils. The array herein described is designed to form the basis for controlling roll, pitch, and yaw. The research performed by Borghi et al. [6], [7] and Kazanskiy et al. [8] on modifying the coefficient of Lift (C_L) of foils across various angles of attack can be used to control both roll and pitch. Their research showed that by using plasma actuators, it is possible to increase the coefficient of Lift by as much as 10%. Using their techniques, the roll could be adjusted by increasing the coefficient of lift of one wing and not the other, while the pitch could be altered by modifying the coefficient of lift of the tail but not the main wing or vice versa. These techniques are further developed in the paper by Pouryoussefi and Mirzaei, which explores the effect the actuator duty cycle has on power consumption and induced mean flow speed. This paper demonstrated that duty cycles as low as 10% could achieve induced flow rates as high as 50% of the maximum while power consumption scales linearly with duty cycles below ~80% [9]. This allows for much more efficient actuation in terms of power consumed relative to induced flow speeds, which is useful since, as was shown by Ferry, plasma actuators are inherently not high efficiency devices [10]. Further, research by Sun et al. showed that, due to hysteresis effects, under certain conditions, the flow remains attached indefinitely once reattached using plasma actuators [11]. To correct for yaw, it would be necessary to modify the coefficient of drag (C_D) on the wings asymmetrically. The research performed by Boesch et al. [12] found that modifying the C_D can be achieved by the firing of plasma actuators against the direction of

flow. Furthermore, the groundwork for such a system was reported by Han et al. [13] in their paper on the applications of plasma actuators to a flying wing and the effects of the asymmetric firing of the actuators. Interestingly, this research showed that it is possible to reduce the overall coefficient of drag by as much as 65% by using plasma actuators pulsed at specific frequencies. This technique might one day allow for overall drag reduction across an airframe covered in an array of PELs. The correction for yaw could come from simply turning off the drag reduction on the wing, which was yawing forwards.

The ability to reduce coefficient of lift and to increase coefficient of drag quickly and without the need to action traditional flight surfaces has additional benefits when considering dangerous stall conditions such as Dutch rolls and deep stalls. In a Dutch roll, a plane yaw, and the forward wing then rolls up. This simultaneously induces more drag and more lift in the leading wing. During the return to normative yaw and roll, the plane can easily overshoot equilibrium and quickly achieve a Dutch roll to the other side. This rolling/yawing motion does not achieve a damped oscillation and can easily become dangerous to the aircraft [14]. One of the major factors in the recovery from a Dutch roll is the response time of actioning the control surfaces. Since plasma actuators require no physical movement, they can be actioned as quickly as the air can respond, producing the fastest possible correction times. Additionally, part of the danger in the case of a Dutch roll is due to the lagging wing gaining too much lift as it yaws forwards. Plasma actuators, unlike flaps, can reduce this effect by modifying the coefficient of drag.

Further safety advantages which pertain to the prevention of stalls and stall recovery have been of particular interest to the research community. The proposed application is to use plasma actuators arrayed to reattach separated flows via re-entrainment of flow over a stalled or near-stalled wing [15]– [19]. Of particular interest has been the placement of plasma actuators near the leading edge or first quarter chord of the wing [13], [20], [21]. This research can be used to increase the overall critical angle for an airfoil by as much as two degrees, as shown by Daud et al. in their paper titled, control of leading-edge separation on airfoil using DBD plasma actuator with signal amplitude modulation [22]. This could be used as a form of emergency flap, which triggers to prevent dangerous near ground, low-speed stalls which can occur during landing. Additionally, research performed by Phan and Shin on reattaching turbulent flows provides a way to reduce the danger of deep stalls, which could allow for reconnection of flow over physical control surfaces despite having fallen into the slipstream of the main wing [23].

One final topic to touch on in this section is the use of plasma actuators to reduce the geometric complexity of wings. This area has been studied both for aircraft and wind turbines.[24] At present, tip vortices induce a significant percentage of the dynamic drag on a modern airframe [14], [25]. Research performed by Boesch et al. provides a way to use plasma actuators firing upstream to reduce the tip vortices and thereby reduce both coefficients of lift and drag[12] which may significantly reduce the dynamic drag of an airframe. Similar research, using direct numerical simulation techniques, was performed by Mizokami et al. specifically for the purpose of modifying C_D and C_L by affecting the wingtip vortices, which is a

convenient way to induce a roll and yaw moment in the wing [26], [27]. Using a system like this can allow for the depreciation of winglets and, therefore, the removal of the weight and form drag of a winglet. Since plasma actuators can be constructed very simply, this can also reduce the construction cost by removing geometrical complexity from the airframe. At this time, it seems prudent to examine where the research stands on the construction of the plasma actuators themselves.

2.3 Physical Design of DBD Plasma Actuators

While plasma actuators are not a new concept, their optimal physical design is still an active area of research. As recently as 2003, Roth published a paper in Physics of Plasmas showing the development of a new type of plasma actuator [28]. That said, while many types of plasma actuators have been tested [29] the most frequently explored and most simply constructed plasma actuator is known as a Dielectric Barrier Discharge (DBD) type. The rudimentary DBD is reliable, solid state, and simple to construct and use. The actuator consists of two metal strips offset with the encapsulated element downstream from the exposed element. These strips are separated by a dielectric, and then a high voltage AC or pulsed DC current is applied across the device. The exposed strip is called the exposed element, and the encapsulated strip is called the encapsulated element. This simplest array is enough to induce plasma actuation when an AC voltage difference in excess of 7kV peak voltage is induced between the actuators [30]. While this simplest array is sufficient, it is not the only option, and many approaches have been taken to improving actuator performance. These fall into three primary areas

the geometry of the actuator elements (how they look from above, as well as the depth and number of encapsulated elements), the effects of arrays of elements in close proximity, and the three-dimensional shape of the elements themselves. Each of these factors has been studied in an attempt to improve the performance of the standard DBD plasma actuator, and promising results have been attained in many of them. In their paper Development of DBD plasma actuators: The double encapsulated electrode Erfani et al. studied the geometry of flat plate electrodes and focused on the case where two encapsulated ground electrodes are present [31]. The team found that for the case where two encapsulated ground-electrodes are used, a streamwise-short (~10mm) and shallow (~0.18mm), electrode just downstream of the exposed electrode, followed by a deeper (~0.5mm) and streamwise-longer (40mm) encapsulated element produced the most body force for a given input power and was able to produce flows up to ~10g*m/s. These results are all considerable efficiency improvements over single encapsulated DBDs, however, they come at the cost of the additional manufacturing complexity of the two encapsulated electrodes. It is also worth noting that because these results focus on efficiency, they did not focus on maximizing peak body force produced by the plasma actuators. Taking a slightly different tack, Corke et al. focused on the production of the maximal peak body force possible using a single DBD (SDBD) [30]. Their research found that a thick dielectric with a low dielectric constant running at higher voltages allowed for maximal body force to be imparted to the flow. This is primarily due to an increased maximal voltage difference between the elements. The typical break-down point of a DBD plasma actuator is when discrete

plasma streamers form which self-entangle and cease to interact effectively with the surrounding fluid. The point where this occurs is directly coupled to the thickness of the dielectric layer between the encapsulated and exposed electrodes. It is of note that this research, which did not concern itself with efficiency, was able to produce body forces an order of magnitude greater than standard plasma actuators, which use Kapton as their dielectric. These results were further backed by the research of Poon et al. in their study that concluded that the dielectric thickness was the most important factor in maximal thrust production [32]. While these researchers were optimizing the SDBD plasma actuators, Moreau et al. were focused on developing arrays of DBD plasma actuators and determining how they interact [33]. This arrangement of actuators is referred to as a multi DBD plasma actuator or MDBD plasma actuator, and they found that MDBDs interfere both constructively and destructively [32]. On the one hand, the cumulative effect of actuators firing together is to increase the entrained flow along the boundary layer and to produce net-stronger jets than possible for a similar number of non-interacting SDBD actuators. On the other hand, the downstream exposed electrodes act repulsively on the flowing plasma and as such retard and detach the flow. The net effect of such an array is none the less to increase net mass flow beyond that of isolated SDBDs equivalent in number to the MDBDs elements. The final geometric consideration is that of the design of the high voltage, active or exposed electrode. In the simplest case, the cross section of the electrode is a simple rectangle. However, since plasma is produced predominantly at and near the surface of the exposed electrode, it has been found that by varying this geometry to produce

higher surface area to volume ratios, it is possible to increase the plasma production efficiency of an SDBD [12]. There are many geometries that have been tried, however, the most successful have been the thin wire [33] Figure 2-2.a and Figure 2-2.c and the saw-tooth Figure 2-2.b and Figure 2-2.d [12] profiles.]

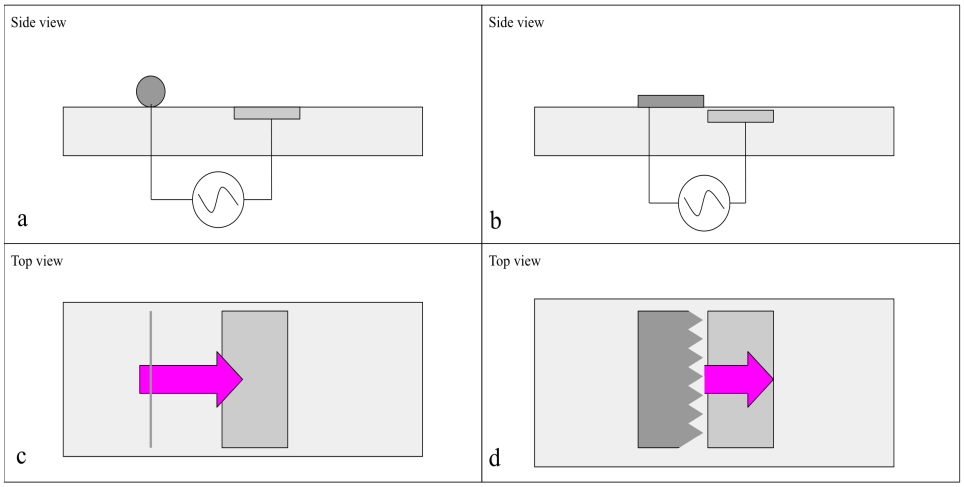

Figure 2-2 (a) A side view of a thin wire Dielectric Barrier Discharge Plasma Actuator (DBD) (b) side view of a saw-tooth Dielectric Barrier Discharge Plasma Actuator, (c) top-down view of a thin wire DBD, (d) side view of a saw-tooth DBD

In the paper mentioned above, Moreau et al. explore both the thin wire and the saw-tooth options. They find that a serrated edge is able to increase the maximum induced velocity in an SDBD by as much as ~30%, while a thin wire produces more thrust across the entire spectrum of potential differences [33]. They further find that the thinner the wire, the more efficient the system becomes. There appears to be a linear relationship between the surface area of the high voltage wire and the efficiency where the radius of the wires varies between 500 μm and 13μm. Further research into saw-tooth exposed elements combined with double encapsulated

elements was performed by Matsuno et al. and proved very successful, yielding up to a sixfold increase in power over standard DBDs [34].While the design of DBD plasma actuators can be highly specialized depending on the goals of the device, the general principles of the device have been laid out by these researchers. Their results suggest that for maximal efficiency at a given voltage, one should aim for double-encapsulated-elements (DEEs) which are as shallow as possible and that the active electrodes should ideally be the thinnest possible wires. Meanwhile, for the maximal thrust possible, one needs deeper encapsulated ground electrodes and thicker dielectrics. Regardless of the desired regime, it is apparent that due to communal entrainment across an MDBD, these arrays are more successful than equivalent SDBDs. Furthermore, considering the fabrication and maintenance challenges of maintaining 13 μm wires carrying high voltage, it is still more beneficial to use saw-tooth active elements in place of their rectangular predecessors. With this understanding of the geometries of plasma actuators and with the goal of fully optimizing the efficiency and thrusting capabilities of these actuators, it is important to explore the driving functions and frequencies providing power to these devices.

2.4 Electrical Considerations for Driving DBDs

The driving function is a critical factor in the efficiency of any plasma actuator, and as such, the design of the voltage waveform has been studied in an effort to maximize the plasma generation of the devices. For instance, Benard and Moreau [34] explored four simple waveforms: the sine wave, positive ramp, negative ramp, and square waveforms. They show that the waveform which produces the greatest

body force is the square waveform. They arrive at this conclusion by inducing a plasma discharge from an SDBD setup with a 20kV bias and a 1 kHz driving frequency. It is possible that at very different frequencies, these results may not hold true, however, for the majority of uses, a frequency in the range of 1kHz is a reasonable value, as can be determined by the fact that most research is performed in the range of a few tens of kHz [20], [35]

The above research provides an idea of what the ideal waveform is, however, additional questions arise around wave amplitude and the regimes of plasma formation as a function of phase. These were studied numerically by Sato and Ohnishi [36]. They studied triangular waveforms and formulated a pair of power laws which describe the production of electrohydrodynamic force as a function of wave amplitude and phase. The two power laws respectively model the 'useful' flowing plasma mode that is of concern, and the 'less useful' plasma streamer regime, which occurs after the critical maximum bias voltage, determined by the dielectric thickness and dielectric constant, are surpassed. They found that, in the regime considered useful, the discharges of plasma are ignited in the negative phase of the triangular waveform and that they are coupled to the surface charge on the high voltage element.

One type of flow not yet discussed but which can be induced through a novel waveform is that of shockwave generation. Research into applications of DBD plasma actuators to high-speed flows has led to research into shock wave formation caused by high amplitude pulses being introduced to SDBDs [37]– [40]. These supersonic shockwaves expand up to several millimeters before dissipating and

appear to be induced by the thermal effects of the highly excited plasma [41]. These shockwaves can be used to introduce tripping points and even to detach flows if necessary. Such devices are typically undesirable for subsonic flows, as flow detachment is considered a problem. However, having more options for flow control is viewed as an asset, and as such, this regime of plasma actuation is mentioned.

From the above research, one can see that there are known and semi-optimized frequency, amplitude, and waveform conditions for the production of a range of desired flows. Having covered the current state of the research into DBD plasma actuators, it is left to discuss the gaps in present research that this work will explore.

2.5 Gaps in Literature

Most research at present focuses on either optimization of thrust via physical or electrical tuning of plasma systems, the study and modeling of the plasma jets themselves, or on the application of specific flow modifications to induce specific desired effects. These are all key areas of research which will improve the function and abilities of plasma actuation systems. However, in terms of applications of plasma actuators, generalist architectures are not widely studied presently. This is not due to a technical inability but due to a focus on producing specific desired effects for specific applications. In order to build more generalized plasma actuator airflow modification systems, it would be useful to be able to produce arbitrary flow modifications near the surface of an airframe or blade. To this end, it would be

useful to induce flow in any direction at any point near a surface in a programmatic way which requires plasma actuators capable of directional control.

Directionally controlled plasma actuators are plasma actuators where the mean direction of the induced thrust can be adjusted without adjusting the physical geometry of the apparatus. Specifically, such devices may be programmed to produce flow in any direction at any time, at any location over a surface. This would allow multiple modifications in rapid succession, the ability to induce the different flow modifications mentioned above, and the general ability to study the effects of multi-directional entrainment and re-entrainment. With such devices, wider applications in control and the generation of programmable flow fields would become possible.

Chapter 3. Methodology

The aim of these experiments is to establish quantitatively the ability to produce near-boundary flows in any direction using arrays of plasma elements. More specifically, the focus is to capture the mean directionality of the flows produced by plasma elements as they cycle through various duty cycle configurations expected to produce a variety of flows. For the purpose of these tests and for simplicity of design square, four directional plasma elements (or fractions thereof) are used. Studying these square plasma elements forms a mathematically and physically simple to understand basis for establishing if the desired level of flow control can be achieved.

These tests' ultimate goal is to establish flow control by producing arbitrary flows within the plane in which the plasma elements are laid out of it. The testing takes place in several steps of increasingly complex flow control. The most basic of these flows is directionally differentiated flow along the primary axes of a plasma element, as shown in Figure 3-1.

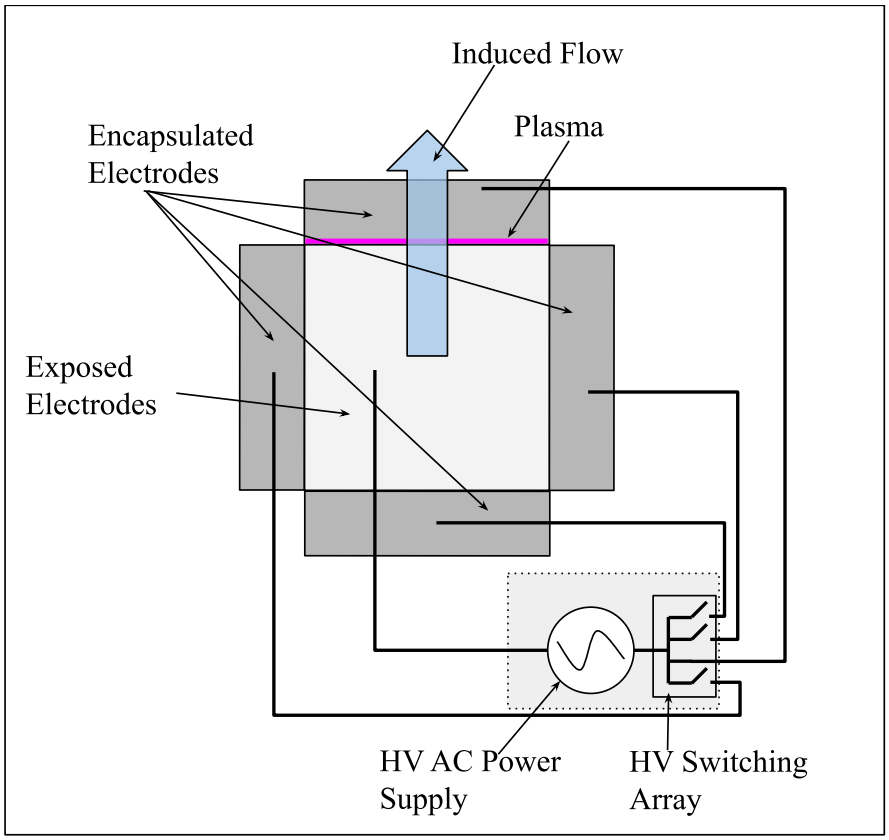

Figure 3-1 A Plasma Element firing in the direction of one of the primary axes of the apparatus.

This is equivalent to activating or "turn on" one of the encapsulated elements while the rest are not active. This test demonstrates the ability of the system to switch between actuators and is equivalent to most of the existing systems in that it produces a flow that is geometrically dependent. The next set of tests establishes the ability to switch between two adjacent encapsulated elements to produce flow in a direction that is not coaxial to the underlying geometry of the plasma element. This is now novel in that the flow is no longer produced in a direction purely determined by the underlying geometry. Such a flow and firing pattern is demonstrated in Figure 3-2 below. Purple regions are where plasma is being

generated as the plasma element fires, and the blue arrow denotes the mean direction of the induced momentum.

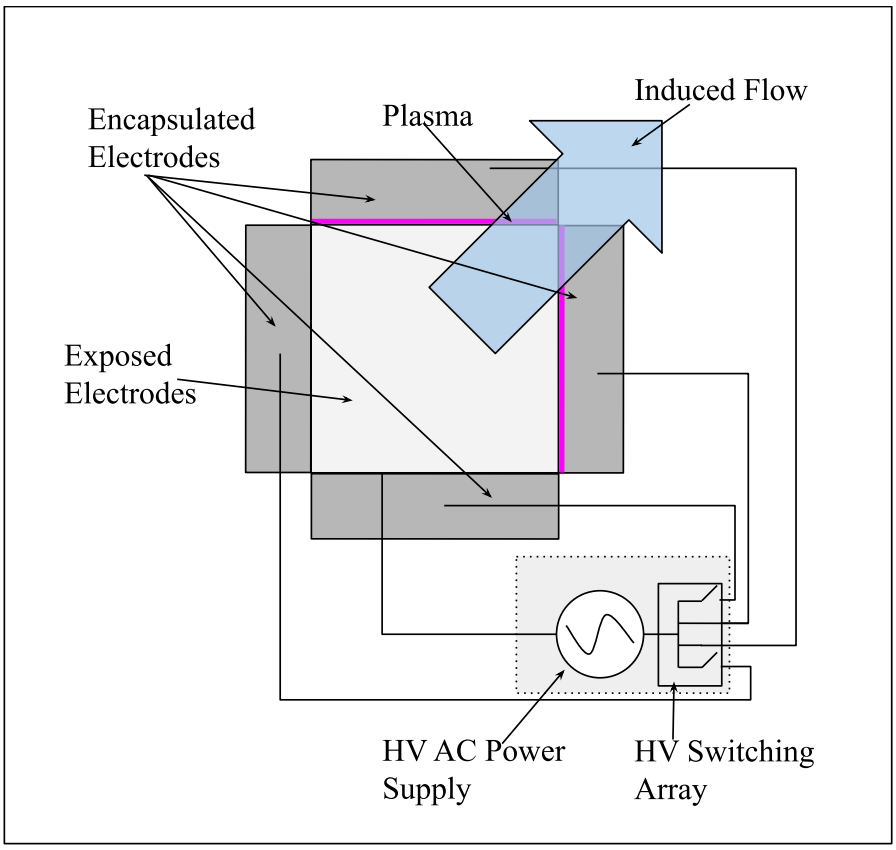

Figure 3-2 A plasma element firing at 45 degrees to the primary axes of the plasma element's geometry by alternating actuation between two encapsulated electrodes.

The off-axis flow continues to show angular resolution for flow at an angle as a function of duty cycles. These tests demonstrate full control over flow directionality in the plain.

The next series of tests focus on the flow out of the plane of the plasma elements. For the first of these tests, a small array of plasma elements is used and flows out of the plane are demonstrated. Figure 3-3 shows the apparatus and firing configuration

required to achieve this result. Purple denotes regions in which plasma is being generated, and blue arrows denote the mean direction in which flow is induced.

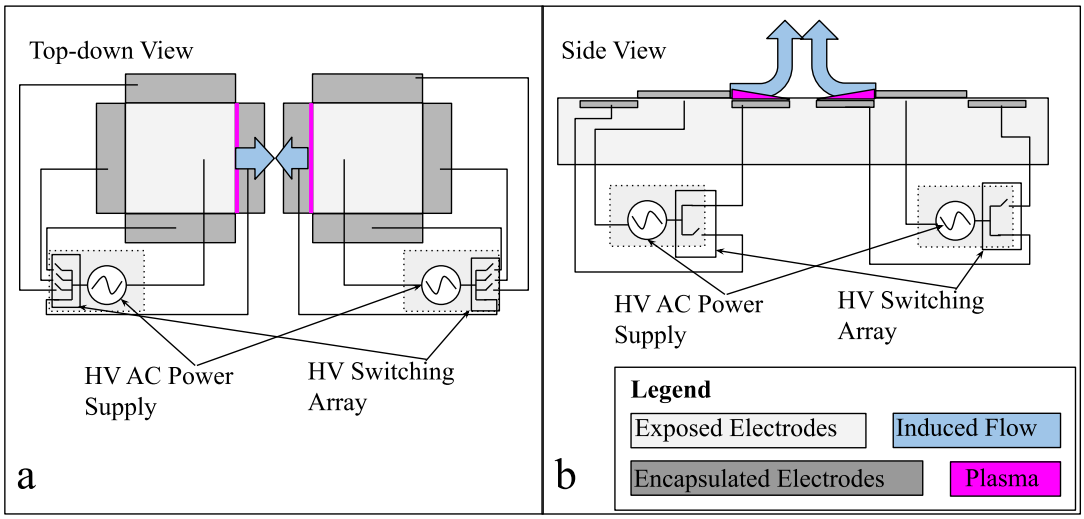

*Figure 3-3(**a**) Top-down view of a small array of plasma elements firing normal to the surface. (**b**) A side view of the same*

This establishes the ability to generate flow normal to the plane of the plasma element array. The next set of tests demonstrates flows at an angle to the surface other than normal and coaxial to the underlying geometry of the plasma elements in the array. Figure 3-4 shows this situation where the purple regions denote plasma actuation within the plasma elements, and blue arrows show the mean direction of induced flow.

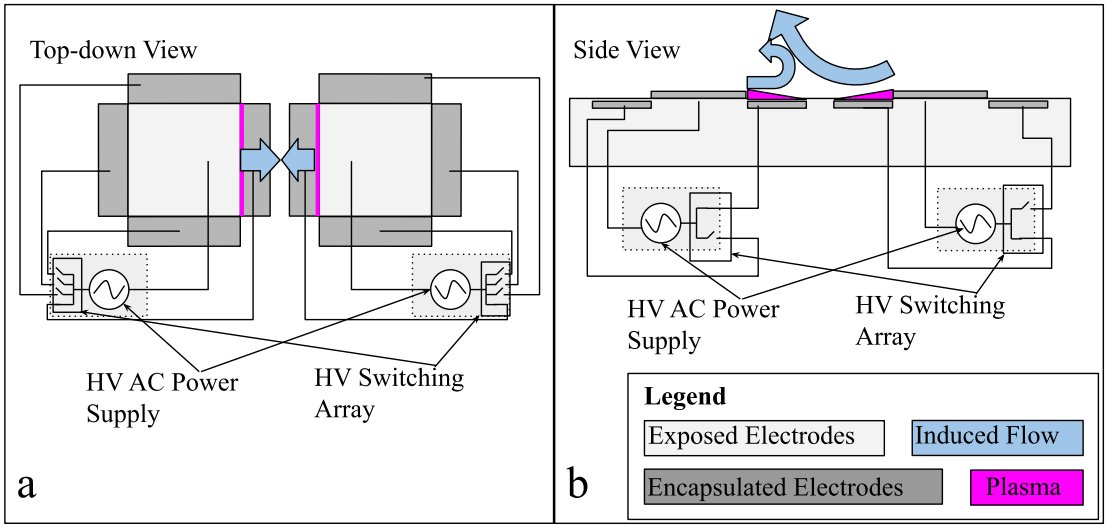

*Figure 3-4 **(a)** A top-down view of opposing plasma elements using differing duty cycles to produce flow out of the plane and not normal to the plane. **(b)** A side view of the same*

The final tests demonstrate the ability of the apparatus to induce flow at an arbitrary angle that is not coaxial to any geometry, as shown in Figure 3-5 below. In Figure 3-5a the purple lines denote the active directions of the plasma elements in the array. The purple arrows denote the mean direction of induced momentum produced by each plasma element in the array, and the blue arrow denotes the mean direction of induced flow from the whole array. Figure 3-5b shows the same situation from a side view; purple regions denote the plasma generated by opposing plasma elements, and blue arrows, again, denote induced flow.

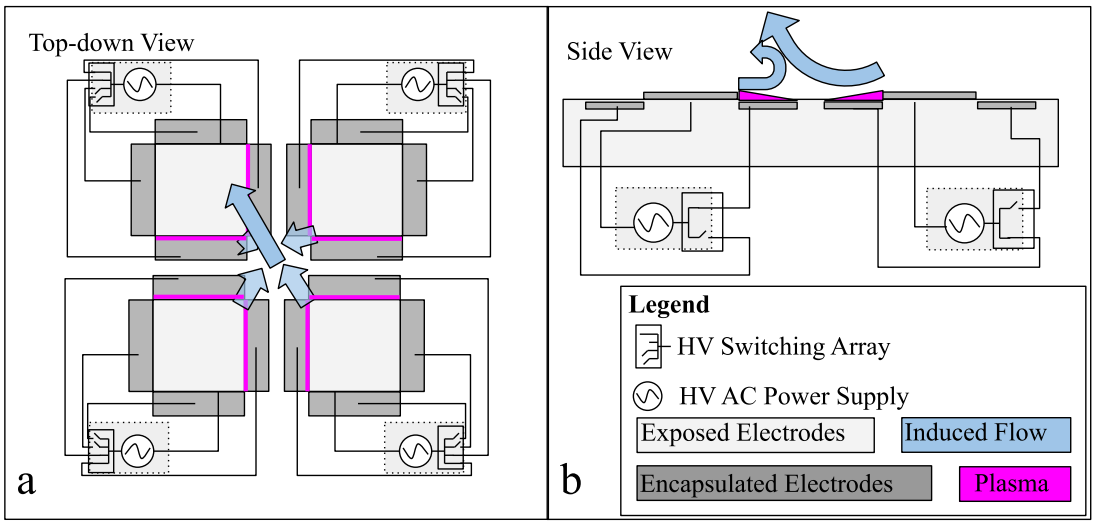

*Figure 3-5 (**a**) An array of plasma elements using differential duty cycles in each encapsulated electrode to induce flow which is not normal to the plane of the array nor coaxial to any geometry of the array. (**b**) A side view of the same.*

With this achieved, it can be concluded that these tests have demonstrated directional flow control sufficient to claim that such an array can reproduce the listed flow effects.

3.1 Software

In order to study the properties of deployed plasma elements in a laboratory setting, it is crucial that tests are highly repeatable. To ensure that the most important variable is controlled in a reproducible manner, the switching array is automated, and the switching is controlled by a microcontroller running custom software. For this purpose, an Arduino Uno running a custom C++ script is used to control the individual switches. This allows control over the frequency and timing of the switching to help avoid burnout. Further, this switching frequency can be precise to

at least two orders of magnitude above the maximum switching rate achievable by the hardware available [42], [43] (see Appendix 1).

The actual software implementation is simple and comprises a C++ script which initializes either two or four General Purpose Input/Output (GPIO) pins which control an h-bridge. The critical elements are to ensure that switching occurs at a given frequency for each of the electrodes and that duty cycles are achieved consistently.

In order to optimize this code, all calculations are done in the initialization of the program, and a simple while(true) loop is used to allow the system to run at maximum speed. All outputs are deterministic, and no “if” or “switch” statements are used during switching, which ensures the Microcontroller (MCU) can optimize its pre-processing. This approach aids in producing predictable output parameters in a device such as this with no internal Real Time Clock (RTC). As discussed earlier, these concerns are negligible as the operation time for such a loop is well below the error in switching time for the physical switches [44].

The script executes code equivalent to the pseudo-code given in appendix 5.1.

In the case of the four plasma elements, a similar code, shown in appendix 5.2, is used to ensure that each switch is switching at the required duty cycle. The delays are adjusted to account for each other, allowing a single thread program to operate multiple switches. This is universally safe, provided the frequency is uniform

between the switches. As frequency effects are outside the scope of this work, this approach can be taken.

For all experiments, the frequency was held constant, and the relevant duty cycles were set. This testing produces a dataset focusing on specific results where the cumulative duty cycles of any two adjacent encapsulated electrodes add to one hundred percent. This is not exhaustive, and certainly, duty cycles summing to any percentage possible (0-200% total DC) could be explored. However, for the purpose of demonstrating the desired flows, this proves adequate and simple to implement.

3.2 Experimental Apparatus

The central novelty of this research is the ability to generate directionally controlled flow from repeating, regular geometry using variable duty cycles to induce directional flow. To establish this, the apparatus must be able to be constructed of materials with exceptionally high dielectric constant, switches capable of medium frequency high voltage switching, and geometries that are easily replicable. With this in mind, the test apparatuses are constructed as square and half-square geometries for the plasma elements tested. These plasma elements are built using self-adhesive copper tape and self-adhesive Kapton mounted on a paper board. When constructing and wiring up the apparatus, it is critical to construct the devices with enough space between electrical elements to ensure no electrical arcing can occur since the voltages are high enough to jump standard small gauge wire insulation.

These test apparatuses are deployed in a calming chamber mounted vertically to avoid interference from thermally induced flows. They are then tested using a particle imaging velocimetry system which comprises a laser sheet, neutrally buoyant reflective oil mist, and a high-speed camera coupled to Davis™ imaging software. The laser illuminates the mist, and the camera captures pairs of images allowing the Davis software to capture flow fields.

3.2.1 Plasma Element Design - Materials Selection

It is necessary that the material selected for the electrodes have a high conductivity to prevent overheating. As such common metals such as copper, aluminum, or steel are most tempting, and in an industrial application, a trade-off between weight, corrosion resistance and appearance will need to be negotiated. For the purposes of this research, copper is chosen as it is a highly conductive, and easily available in a self-adhesive foil tape with a thickness of 0.1 ± 0.05 mm.

The material chosen as the dielectric is much more important for performance. The selected material must have a large dielectric constant so that a thin film will be sufficient to withstand the voltage required to induce the dielectric breakdown of air. Specifically, since the dielectric constant of STP air is ~1, the solid dielectric must have a dielectric constant sufficient to induce the breakdown of the air before undergoing electrical breakdown. The material must also be sufficiently resistant to heat so as to not melt or erode quickly under the sustained plasma sheet. Finally, a material that is easily manipulable is desired to facilitate construction and wiring manipulation during testing.

After consideration of the various materials commonly available which would provide the required attributes, the test plasma elements were constructed from Kapton tape. Kapton displays a sufficiently high dielectric constant, at over 3, and it has a maximum operating temperature of over 360 degrees Celsius which is sufficient to withstand the expected maximum temperatures of ~200 degrees Celsius which have been observed in DBD discharges by Dong et al. [45]. The relevant mechanical, thermal, and electrical properties of Kapton are displayed below [46].

Material	**Dielectric constant**	**Maximum operating temperature [oC]**	**Notes**	**Selected**
Kapton	3-3.8	360-410	Standard selection in most tests	Yes

Table 3-1 Properties of selected dielectric material (Kapton)

3.2.2 Plasma Element Design – Geometry

A Plasma Element (Pel) is a single, directionally controllable dielectric barrier discharge plasma actuator. Each Pel comprises a dielectric barrier discharge plasma actuator featuring three or more encapsulated electrodes about a central exposed electrode. These encapsulated electrodes must be spatially distributed in such a way so that the mean vector normal to their common edge with the exposed electrode produces a set of axes which form a positive basis for the plane of the array. That is to say that through the addition of non-negative multiples of the averaged normal vectors, all points in the plane of the array must be reachable. This ensures that flow may be produced in any direction within the plane of the apparatus.

Figure 3-6, shown below, displays three representative example geometries for acceptable Pel designs. For each of these geometries, the average vector normal to the interface between the encapsulated (dark grey) and exposed (light grey) electrodes forms an additive basis for a plane.

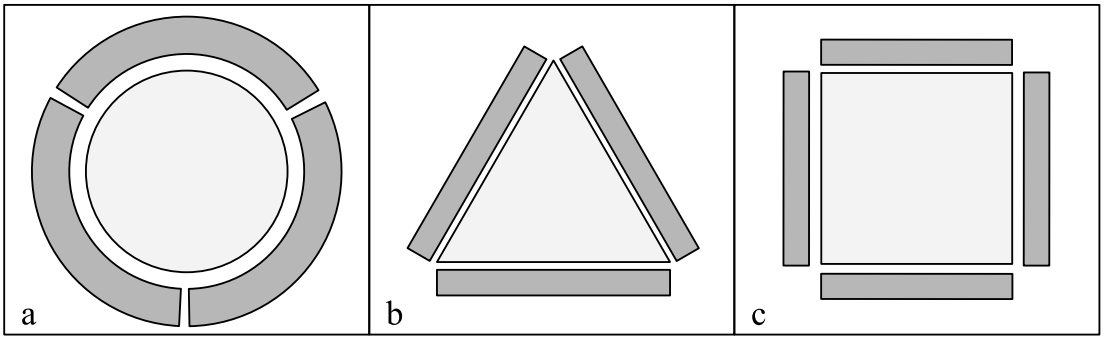

Figure 3-6 6 Three representative acceptable plasma element geometries

e.

Figure 3-6.a displays a circular three-element PEL, Figure 3-6.b shows a similar construct with triangular three element PELS and Figure 3-6.c shows the square shaped four element array, which is primarily studied in this thesis.

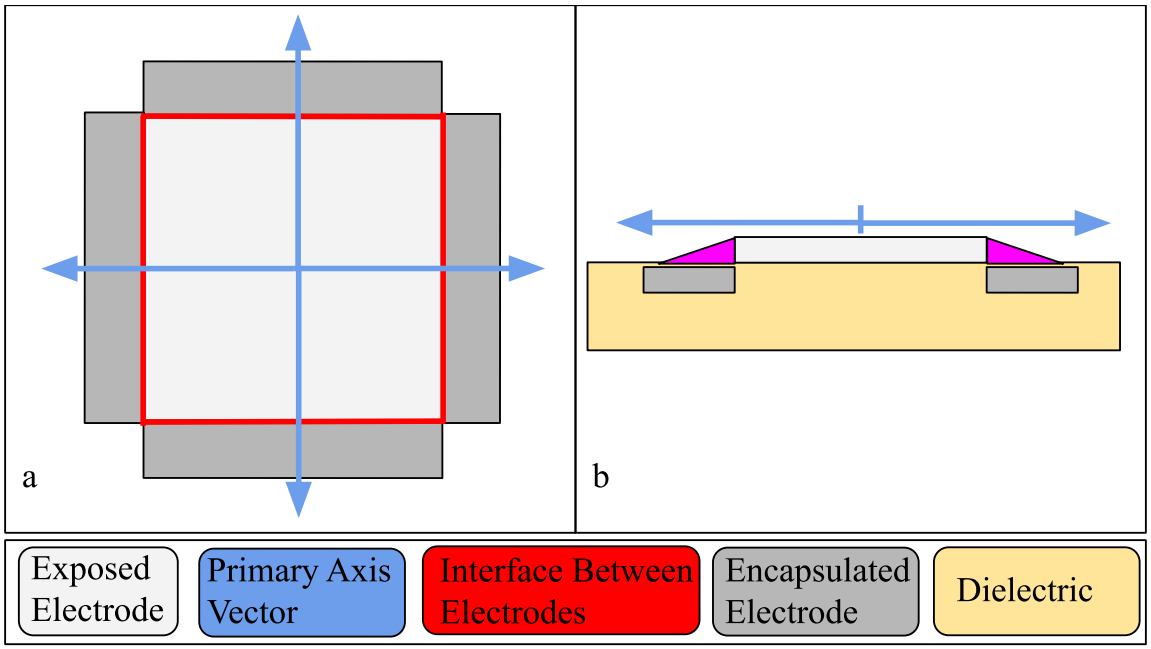

*Figure 3-7 **(a)** The interface between encapsulated and exposed electrodes in red, resultant primary axis vectors in blue. **(b)** Side view of the apparatus which shows induced plasma and primary axis directions*

Figure 3-7 shows the interfaces between the exposed electrode (light grey) and encapsulated electrodes (dark grey) as a red line. The vectors normal to these interfaces are superimposed in blue, showing the primary axes of one example geometry. Figure 3-7.b shows a side on view of a cross section of the geometry in figure 3-7.a. In this figure we show the direction of induced plasma which determines the direction of the primary axis vector. When these primary axes intersect at a common point it is apparent from some simple linear algebra that these form a basis for a space.

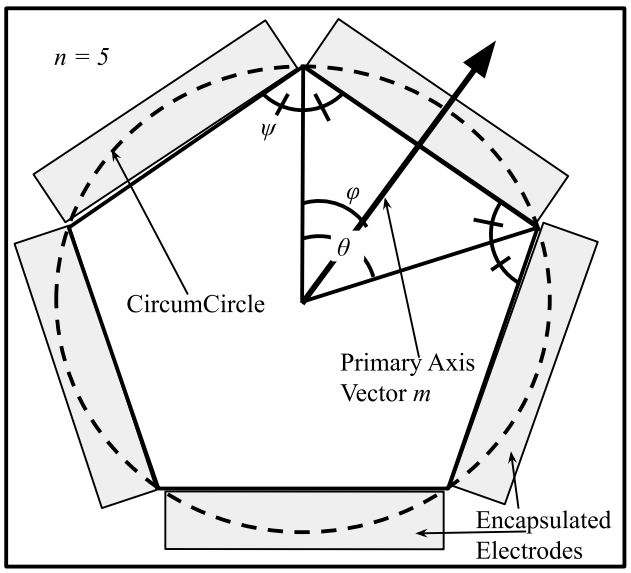

Figure 3-8 A pentagon for the purpose of demonstrating that regular convex polygons produce curl-less primary axes. In such geometries this polygon will form the exposed electrode

For a given geometry based on an *n* sided regular convex polygon, such as that shown in figure 3-8, the primary axes can be represented as *n* vectors normal to the faces. Each face of a regular convex polygon describes a chord of a circumcircle for that polygon meaning all normal vectors bisecting that face originate at the center point of the circumcircle which can be shown via proof by contradiction. Additionally, it is assumed that the steady state electromagnetic field produced between the plates of the plasma actuator is normal to the line of intersection between the encapsulated and exposed electrodes and is symmetric about the mid-line of the encapsulated electrode. This assumption is in line with existing dielectric barrier discharge literature, which models DBD plasma actuators similarly to parallel plate capacitors, and is born out by experimentation. Figure 3-9 below shows actuation of a plasma element in one direction demonstrating flow which is directionally isolated to the direction normal to the interface between the encapsulated and exposed electrodes.

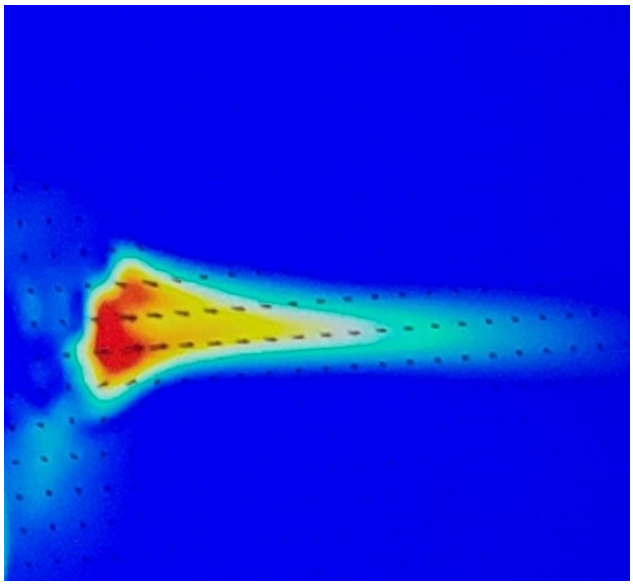

Figure 3-9 Isolation of flow direction in the direction normal to the interface between encapsulated and exposed electrodes and in the direction of the encapsulated electrode.

Knowing that these vectors originate at the center point of the circumcircle it is possible to define the m^{th} basis vector in polar coordinates as the unit vector in the direction φ where φ is defined in degrees as

Symbols used in the calculation of the basis vectors	
φ	The overall angle of the basis vector in question
θ	The angle between basis vectors
m	The specific basis vector we are considering (range = [0,n))
n	The number of edges in the regular polygon

Table 3-2 The symbols used in the calculation of the basis vectors.

Equation 3-1derivation of the angle of the m-th basis vector for a regular convex polygon exposed electrode geometry

$$\varphi = \mathrm{m}\theta + \frac{\theta}{2} = \theta\left(\mathrm{m} + \frac{1}{2}\right)$$

$$= (180 - 2\psi)\left(\mathrm{m} + \frac{1}{2}\right)$$

$$= \left(180 - 2\left(\frac{1}{2}\left(180\frac{n-2}{n}\right)\right)\right)\left(\mathrm{m} + \frac{1}{2}\right)$$

$$= \left(180 - \left(180 - \frac{360}{n}\right)\right)\left(\mathrm{m} + \frac{1}{2}\right)$$

$$= \left(\frac{360}{n}\right)\left(\mathrm{m} + \frac{1}{2}\right)$$

$$= 360\frac{m}{n} + \frac{180}{n}$$

Describing this in cartesian coordinates we find that the m^{th} basis vector can be described by the following equations:

Equation 3-2 Cartesian coordinate vector for the m-th basis vector for an exposed elctrode with n faces

$$\boldsymbol{V}_m = \langle \cos\left(\frac{360m + 180}{n}\right), \quad \sin\left(\frac{360m + 180}{n}\right) \rangle$$

Thus the vector field can be described by the linear combinations of these basis vectors.

There are an infinite number of acceptable geometries limited only by the requirement that the normal vectors span the subspace describing the plane in which the plasma actuator is situated. That is all points in the plane of the plasma actuator can be reached by some positive combination of the basis vectors.

As the purpose of this research is to describe the directional control of such apparatus the specific geometry is not critical so long as it adheres to the above requirements. As such a simple square geometry is selected for our experimentation as it forms nice vectors within cartesian coordinates and is simple to construct. These results should be similar for all geometries satisfying the requirements outlined.

Regarding the sizing of the apparatus the devices are not expected to be sensitive to size other than the down stream gap between the exposed and encapsulated electrodes. As such this gap is held at 0 ± 100nm horizontally and 0.1 ± 0.05mm vertically. When constructing arrays of plasma elements, it is necessary to ensure that enough dielectric exists between isolated electrical components to prevent arcing. As the encapsulated electrodes are the component closest to each other it is critical that these remain far enough apart to prevent arcing through the dielectric. In order to control where cold plasma generation (shorting) occurs it should suffice to ensure all gaps between encapsulated electrons are at least as large as the gap between the encapsulated and exposed electrodes. All other size constraints are not expected to have significant effect on the performance of the plasma elements when considering only directionality.

The remainder of this chapter will focus on the design used in our experiments, which is the four encapsulated-element square shaped PELs corresponding to a case of the geometry outlined in Figure 3-6.c.

The first step in studying this apparatus is to establish the ability to differentially control induced flow in a plasma element. To this end, the geometry shown in

Figure 3-10, was constructed, and studied. Figure 3-10.a shows a diagram of the geometry studied with measurements, while Figure 3-10.b is a picture of the apparatus.

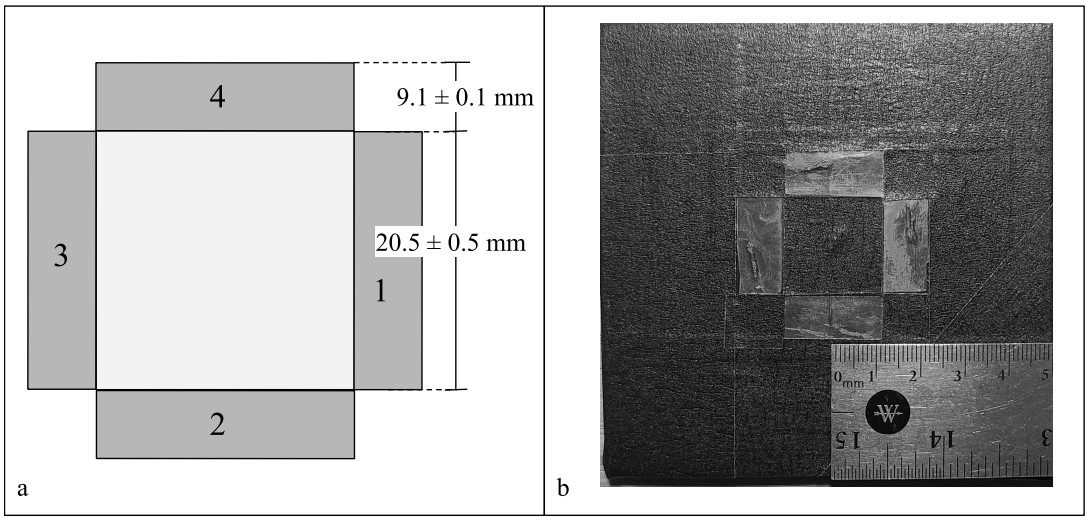

*Figure 3-10 (a) A diagram of the plasma element studied for controllability proof of concept, (**b**) a picture of the studied apparatus referred to hereafter as test geometry 1*

The specific geometry of the PEls studied in this research is shown in Figure 3-10. There were three different apparatuses used during this research, and error margins account for the variance between these apparatuses. All apparatuses follow a simplified version of the same general geometry as outlined above in Figure 3-6.c. A simplified two-encapsulated plasma element is also constructed and tested. This geometry is easier to test in the physical apparatus. Using this simplified PEl it is possible to demonstrate the degree of control over the direction of induced momentum within the quadrant of the vector field described by the primary axes of the device, in this case, a one-quarter plane. This is sufficient to show control over flow within one-quarter of the available directions. Once it is demonstrated that this apparatus is able to produce arbitrary flow within the quadrant corresponding to its

primary axes, it is possible to claim that a full plasma element with primary axes forming an additive basis for the required vector space will be able to induce flow in an arbitrary direction. While there are clearly non-linearities in the interactions of such flows, for the purposes of this research, only flows induced by one or two adjacent directions are considered. Therefore, selecting any two adjacent axes in a plasma element is equivalent, and the proof of control over one quadrant (in a square geometry such as that described in Figure 3-10) is equivalent to the proof of control over the entire space of in-plane flows.

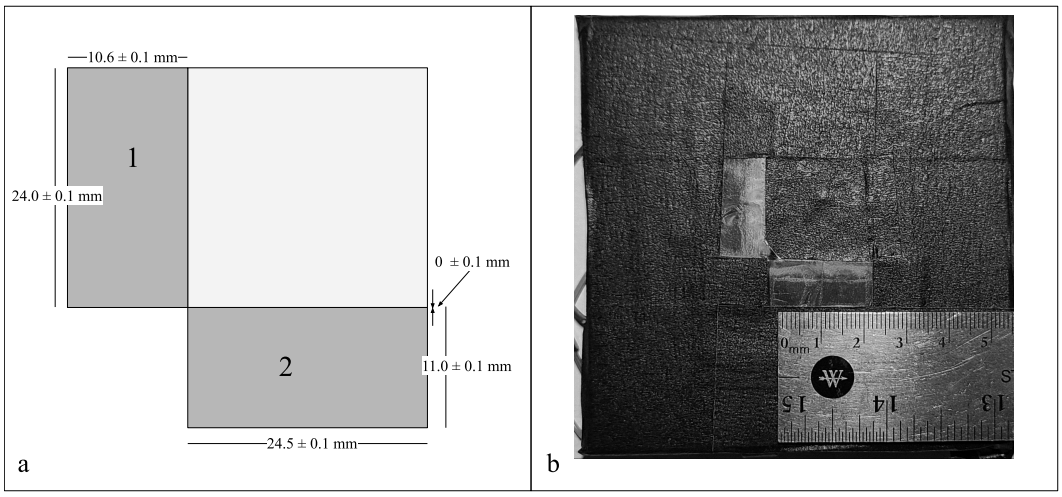

Figure 3-11 Actual dimensions of plasma elements tested during this research, referred to hereafter as test geometry 2.

3.2.3 Array of Plasma Elements Design - Array Geometry

This research will show that the apparatus outlined above, a single plasma element, is sufficient to generate arbitrary flow in the plane of the apparatus. However, to claim reproduction of the listed flow modifications, it must be possible to induce flow out of the plane of the apparatus as well as within it. This research goes on to

show that by combining multiple plasma elements, it becomes possible to induce arbitrary flow directions.

We say such an array is homogeneous when all the plasma elements within it are identical up to the position, meaning that each element has the same geometry, wiring, and orientation in the array. In a homogeneous array, each region is equally able to generate any desired flow. Since each region can generate arbitrary flow direction, and since all regions in the array geometry are equally able to generate the same flows, such an array allows for fully programmable flow near the surface of a homogeneous array of plasma elements. Figure 3-12 displays an example array of plasma elements that can generate such behavior.

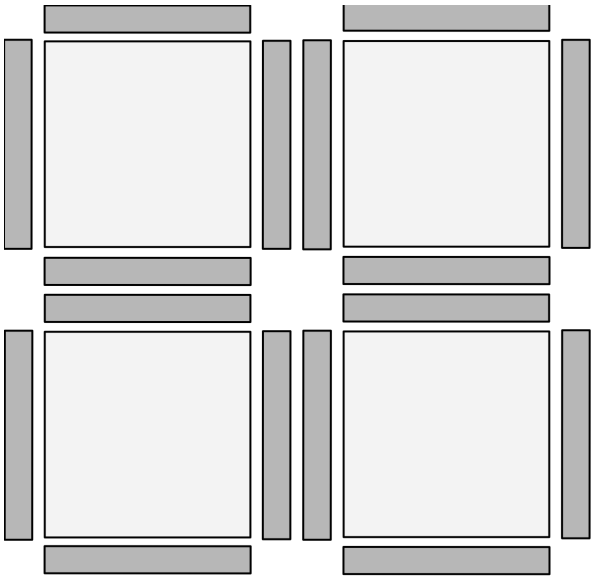

Figure 3-12 An example array of plasma elements with four primary axes

In order to simplify the geometry under study, an array was built in which only the encapsulated electrodes pointing inwards within the simplified array were retained. This is shown in Figure 3-13. This small array is able to generate inter-element

effects by having plasma elements produce opposing flows. These opposing flows are studied to determine the level of control that can be achieved over the direction of the flows out of the plane of the array.

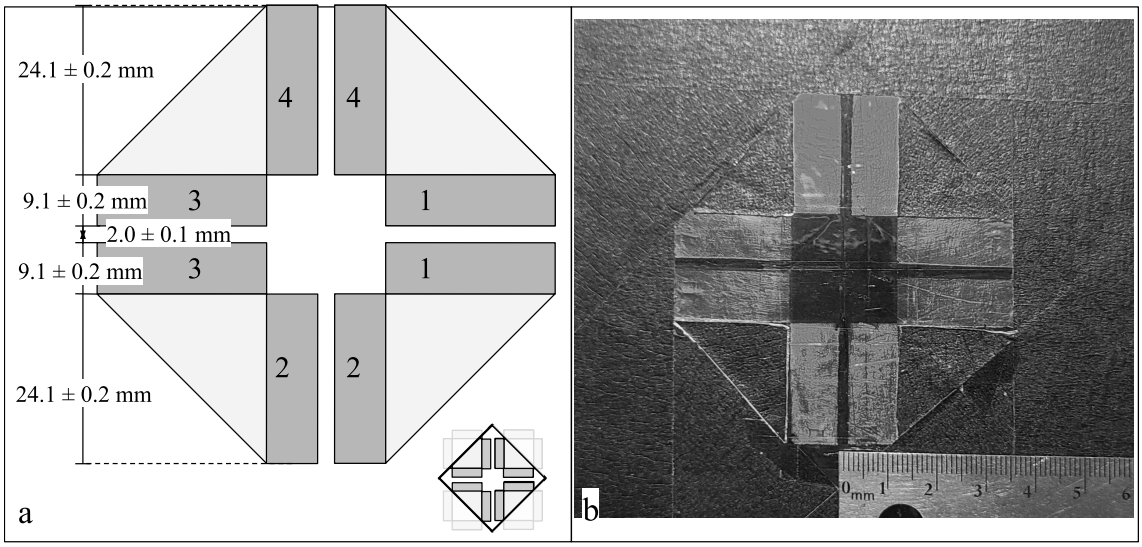

*Figure 3-13 (**a**) Diagram of a small array of plasma actuators studied for control of flow out of the plane, the inlaid figure shows the test apparatus as part of a larger array, (**b**) a picture of the apparatus referred to hereafter as test geometry 3.*

3.2.4 Plasma Element Design - Electrical Considerations

Plasma elements are ultimately governed by the same principles as standard dielectric barrier discharge plasma actuators. To this end the actuators only begin to function above a specific voltage known as the breakdown voltage (V_B). As discussed in equation 2-1, this voltage can be determined from Paschen's law. Assuming no secondary emission from the exposed electrode, it is possible to simplify Paschen's law to

Equation 3-3 Paschen's Law without Secondary Electron Emission

$$V_B = \frac{Bpd}{\ln(Apd)}$$

Where the symbols are the same as those given in table 2-1

For a gap of 0.1mm as in the case for these experiments where the apparatus uses a 0.1mm thickness Kapton tape with no horizontal gap.

Equation 3-4 Minimum breakdown voltage for experimental geometry

$$V_B = \frac{2737.50 \bullet 10^5 \bullet 10^{-4}}{\ln(112.50 \bullet 10^5 \bullet 10^{-4})} = 3896.5V \sim 3.9kV$$

Symbols used in Paschen's Law	
V_B	Breakdown voltage [V]
A	Saturation Ionization [1/(kPa•cm)]
p	Pressure [Pa]
d	Gap distance [m]
B	Experimental Constant [V/(kPa•cm)]
γ_{se}	Secondary electron emission coefficient

Table 3-3 Variables used in Paschen's Law

As such it is apparent that the minimum voltage for the actuation of the tested plasma actuator is >3.9kV. In order to account for experimental error such as humidity, variance in temperature and pressure, and imperfections of the materials under test a value of approximately 7kV is selected.

3.2.5 PIV System & Measurement Procedures

In order to make quantitative measurements of the flow modification generated by such apparatus, it is necessary to use particle imaging velocimetry (PIV) techniques to capture flow field averages. This allows for the study of the stable effects

generated by these apparatuses, which are the primary focus of this research. During experimentation, an apparatus (shown in Figure 3-14) was used consisting of an atmosphere calming chamber (3-14.1), a test-bed containing any of the test geometries (3-14.2), a laser(3-14.3) capable of producing a high power laser sheet (3-14.4), an apparatus for generating neutrally buoyant smoke which is reflective to the laser light(3-14.5), a high speed camera synced to the laser(3-14.6), a computer running PIV software(3-14.7), a power supply (mains power is used)(3-14.8), a variac for power management and tuning(3-14.9), a high voltage AC transformer(3-14.10), a computer running Plasma element control software(3-14.11), and an array of high voltage switches(3-14.12) designed to isolate the encapsulated electrodes in the test geometries. Figure 3-14.a shows these elements in a diagram for clarity, and Figure 3-14.b shows a picture of the experimental setup labeled appropriately. Relevant part numbers and manufacturers are available in Appendix 2.

The experimental design focuses on isolation of flows generated from the plasma elements and arrays thereof. The calming chamber is necessary to ensure the atmosphere is able to reach full quiescence before each test run. The experimental test bed is held vertical for initial tests to isolate thermal flows in the positive y direction while measuring electrohydrodynamically induced flows in the positive x direction. The laser sheet and camera are aligned to capture induced flow and any thermal effects. The test bed can be re-aligned in small increments (~0.1mm) to allow for a variety of test slices to be taken for later interpolation. The Variac and high voltage power supply ensure that ~7kV are delivered to the plasma elements under test. The result is not expected to be sensitive to the voltage provided that

the voltage is greater than the breakdown voltage for the given device. This is because all directions of the plasma element share a common encapsulated electrode and power supply ensuring they experience equal voltage due to Kirchhoff's law.

High voltage switches and associated control electronics are coupled with a microcontroller running custom software to mange duty cycles. This allows a controlling computer to program in different flow regimes by modifying the duty cycles of various encapsulated electrodes.

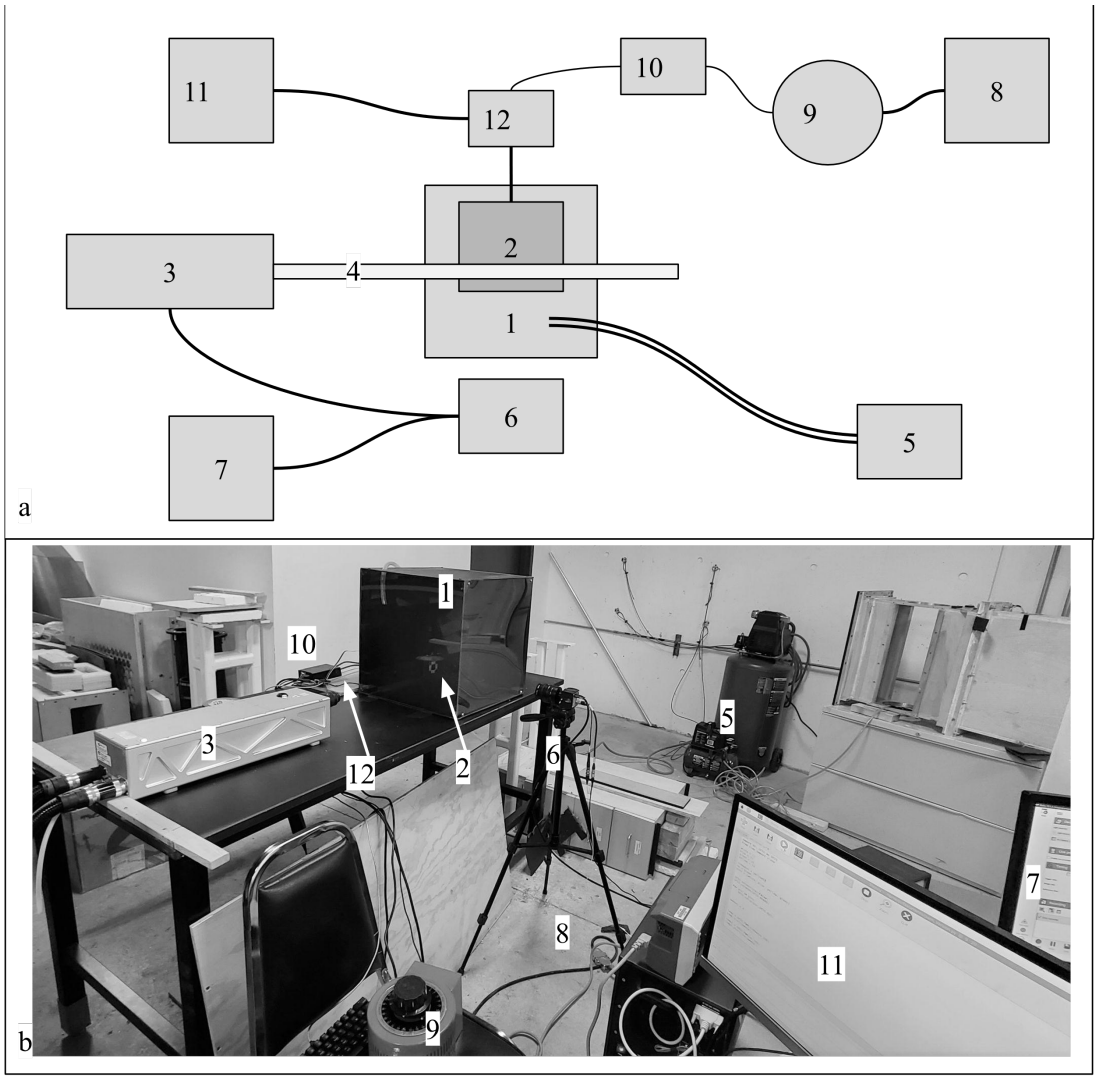

*Figure 3-14 (**a**) Block diagram of experimental setup in lab. (**b**) Picture of experimental setup in lab*

3.3 Experimental Test Regimes

There are four major test regimes undertaken in this research with four distinct goals for proving control over the flow near the apparatus. The first goal is to demonstrate control over a plasma element by demonstrating flow coaxial to one primary axis of the underlying plasma element when isolating all but one encapsulated electrode. This goal is achieved through the study of test geometry 1. The second goal is to show control over the flow within the plane of the array. This

is done by varying the duty cycles of the encapsulated electrodes to induce flows that are not coaxial to the primary axes of the plasma element. To test this capability, test geometry 1 is also used. Finally, the third goal is to demonstrate flow out of the plane by firing opposing plasma elements toward each other. In order to demonstrate arbitrary flow control in any direction out of the plane, test geometry 3 is used, and the duty cycles of each of the opposing encapsulated electrodes are varied. Taken together, the demonstration of these four domains of control covers the space of possible flow directionality and suffices to support the claim that such an array can produce the desired flows near the surface of the array.

3.3.1 General procedure

While the specific test regimes require specific geometry and test geometries, many elements of the test regime are shared. For all tests involving duty cycles, a constant frequency of 100Hz was used. In each test, the air calming chamber was allowed to settle until no air movement was visibly apparent before the test began. During each test, the test geometries under test were energized and allowed to run for several seconds to achieve a steady state before testing began. Then one hundred pairs of images were taken using the high-speed camera. After all, tests were run, the test geometry was shifted with respect to the laser sheet to capture slices of the flow at multiple depths. For each slice, the image pairs were then extrapolated into flow fields which were averaged, interpolated across the axis of the slices, and graphed. Duty cycles for each of the tests can be found in the corresponding sections of Appendix 3.

3.3.2 Control coaxial to the primary axes of the device

In order to demonstrate basic control over a single plasma element, all but one encapsulated electrode is isolated by not wiring the other encapsulated electrodes into the AC circuit. This leaves all but one encapsulated electrode as floating components. This apparatus is placed in the test chamber, as demonstrated in Figure 3-15 below. The apparatus is placed vertically and imaged at multiple depths of the surface shown in Figure 3-15 to allow 3d interpolation in the data post processing. All tests were conducted with flow pointed horizontally to ensure thermal conduction was not a major factor in inducing flow.

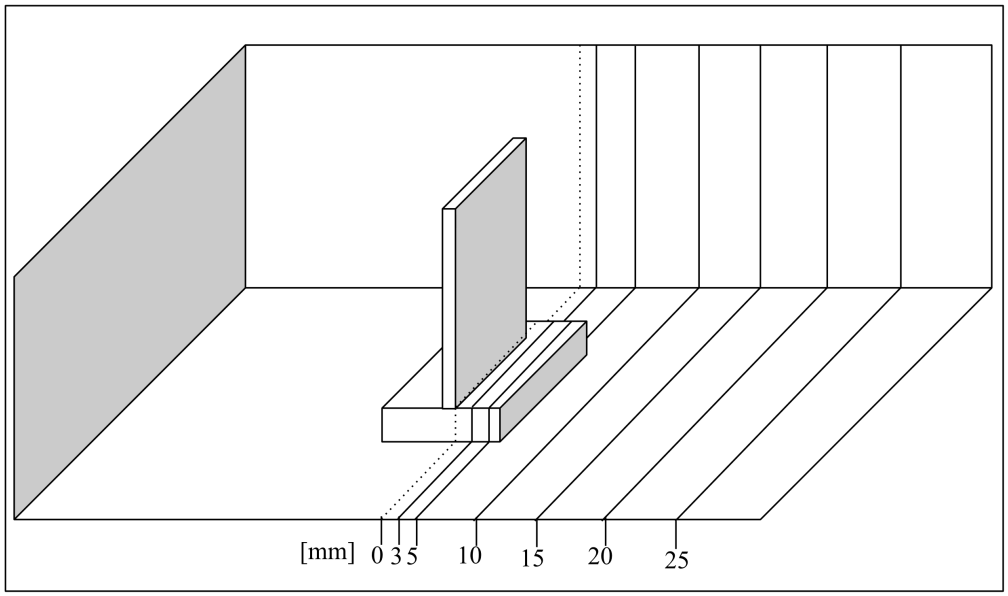

Figure 3-15 Diagram showing location of laser sheet illumination for testing basic differential control with plasma configuration 1.

Table 3-4 shows sample test regimes which were undertaken to determine if it was possible to isolate the direction of flow generated by the plasma actuators. For these primary tests it suffices to use 100% duty cycle in one direction encapsulated electrode and 0% in all others. To provide evidence of symmetrical action two different tests are conducted with adjacent encapsulated electrodes actioning.

Test Geometry	**Purpose**	**Duty Cycle [%] of Encapsulated Electrode…**			
		1	**2**	**3**	**4**
1		100	0	0	0

	Establish differential firing control	0	100	0	0
	Establish Symmetry of firing action for different encapsulated electrodes	100	100	0	0

Table 3-4 The duty cycles of encapsulated electrodes from test geometry 1 (figure 3-10) used to establish that actuation can be isolated to any individual or subset of encapsulated electrodes.

3.3.3 Arbitrary control within the plane of the device

With the above tests establishing differentiated control over the direction of flow induced by a plasma element, it is now necessary to establish control over the flow within one-quarter plane. Figure 3-15 shows the configuration of the testbed for these tests. The plasma element is placed vertically in the test chamber, and readings are taken with the laser sheet at the locations noted in Figure 3-15. During these tests, the plasma actuator previously shown in Figure 3-11 is used in combination with the switching array, which varies the adjacent encapsulated electrodes duty cycles. Such an actuator is only capable of inducing flow within one-quarter of the plane since it is only half of a normal plasma actuator and, therefore, only has two principal axes. However, since all plasma elements described above must be symmetrical, no directions are considered special, and consequently, the selection of two adjacent encapsulated electrodes is arbitrary. As such, demonstrating arbitrary control over the direction of flow in the space described by the primary axes of the plasma element suffices to show that arbitrary flow control is possible when sufficient base vectors are present in the geometry of the plasma element.

To begin, test geometry 2 was placed horizontally in the test bed, as shown in Figure 3-16. Then, to establish control over direction within the plane, tests are

completed wherein two encapsulated electrodes were fired differentially to adjust the mean direction of induced flow. Readings were taken at a variety of distances from the center of one of the interfaces, as shown in Figure 3-16.

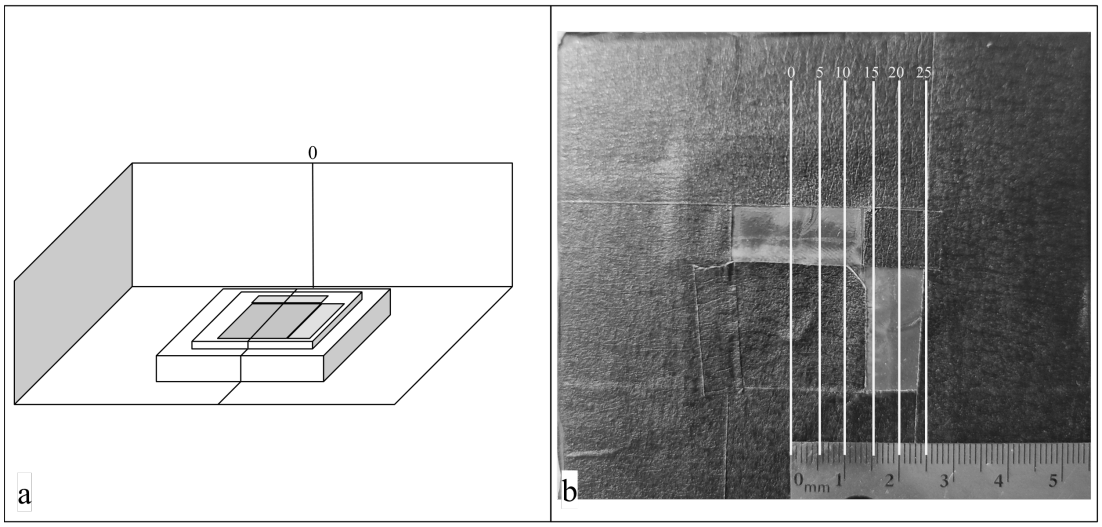

*Figure 3-16 (**a**) Diagram of orientation of test bed. (**b**) location of laser sheet during consecutive tests*

The regime of tests progresses in increments of five percent for the control variable, the duty cycle. To begin, one electrode was set to one hundred percent duty cycle while the other was set to zero. In increments of five percent, the duty cycle of electrode one was decreased while the duty cycle of electrode two was increased by the same percentage. The test was repeated at several depths, shown in Figure 3-16, to establish a three-dimensional dataset of the average flow. In each test, the process described in Section 3.3.1 was undertaken to capture a quantitative measurement of the average flow induced. Table 3-5 contains the duty cycles of the encapsulated electrodes during this phase of testing.

Section	**Test Geometry**	**Purpose**	**Duty Cycle [%] of Encapsulated Electrode…**

			1	2	3	4
3.3.3	2	Arbitrary flow within the plane of the array	50	50	-	-
			55	45	-	-
			60	40	-	-
			65	35	-	-
			70	30	-	-
			75	25	-	-
			80	20	-	-
			85	15	-	-
			90	10	-	-
			95	5	-	-
			100	0	-	-

Table 3-5 The duty cycles of encapsulated electrodes from test geometry 2 (figure 3-11) used to establish control over flow direction within one quarter plane.

3.3.4 Control out of the plane

This test regime focuses on demonstrating arbitrary flow out of the plane of the array. Test geometry 3 is placed in the test bed horizontally. Initial proof of concept tests is run with all four plasma elements configured to run with a 100% duty cycle. The flow is imaged at several distinct locations on the plasma configuration, as shown in Figure 3-17.

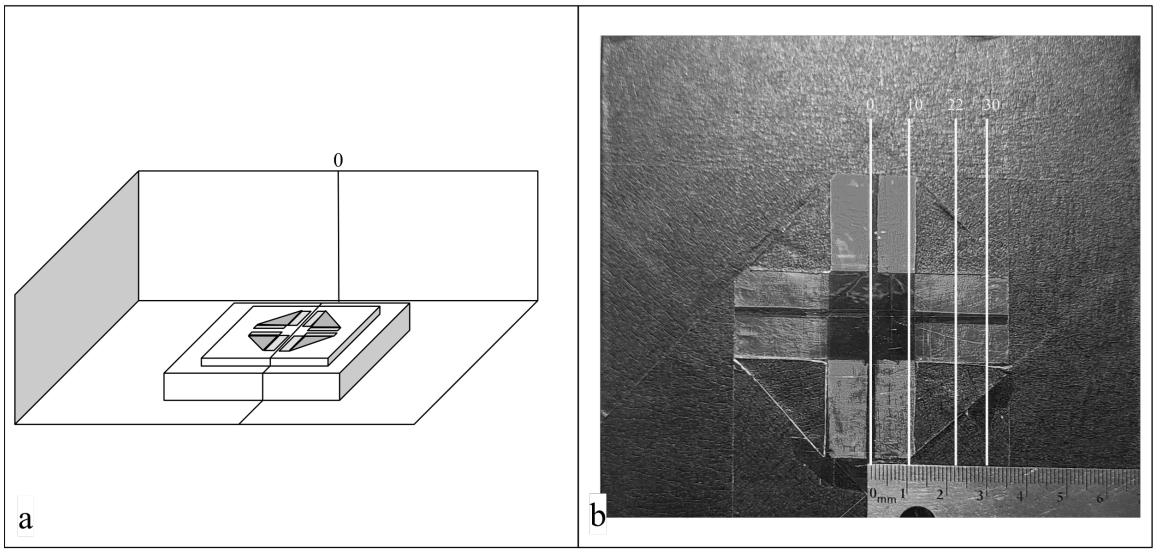

*Figure 3-17 (**a**) Diagram of orientation of test bed with zero marked. (**b**) Image of plasma apparatus three with location of plasma sheets noted*

To further understand control overflow out of the plane that is not fully normal to the plane, the plasma configuration was structured as two pairs of opposing plasma elements. Similar to Section 3.3.3, the opposing pairs of plasma elements are energized to produce average flows out of the plane at an angle other than at right angles. Such flow is still coaxial to the primary axes of the array in the plane of the array. Table 3-6 below shows the duty cycles used in the testing to establish control over the azimuthal angle of the mean flow. The encapsulated electrode numbering corresponds to the numbering in figure 3-13.

Section	**Test Geometry**	**Purpose**	**Duty Cycle [%] of Encapsulated Electrode…**			
			1	**2**	**3**	**4**
3.3.4	3	Establishing flow out of the plane	100	100	100	100
		Measuring control of azimuthal angle	50	0	0	50
			50	5	5	50
			50	10	10	50
			50	15	15	50
			50	20	20	50
			50	25	25	50
			50	30	30	50
			50	35	35	50
			50	40	40	50

Table 3-6 The duty cycles of encapsulated electrodes from test geometry 3 (figure 3-13) used to demonstrate control over the azimuthal angle of flows generated out of the surface

Finally, to establish flow out of the plane at an angle that is not normal to the plane and is not coaxial to the geometry of the plasma element, plasma elements were

energized differentially to demonstrate arbitrary flow control out of the plane. Table 3-7 shows the duty cycles selected for this testing. These duty cycles are selected to isolate modifications to single encapsulated electrodes or pairs of opposing encapsulated electrodes in each subsequent test. The aim of this is to show the difference in resultant flow field which can be caused by modifying individual actuator duty cycles in a multi-actuator effect.

The numbering in table 3-7 corresponds to the numbering shown in figure 3-13.

Section	**Test Geometry**	**Purpose**	**Duty Cycle [%] of Encapsulated Electrode…**			
			1	**2**	**3**	**4**
3.3.4	3	Displaying flow that is at an angle to the plane, the vertical axis, and all actuator geometry	50	45	45	50
			50	50	50	50
			50	50	20	50
			50	45	25	50
			50	40	30	50
			50	35	35	50
			50	50	25	45
			50	50	30	40
			50	50	35	35

Table 3-7 The duty cycles of encapsulated electrodes from test geometry 3 (figure 3-13) used to demonstrate completely non-coaxial flow generation

3.4 Data Processing

3.4.1 Raw images to velocity fields

The raw data comprises collections of sets of image pairs corresponding to the pairs of images captured by the high-speed camera. Using the Davis software to post-

process the images results in collections of flow fields. In this case, since the induced flows are not optimized for speed, it is critical to allow for the measurement of low-speed flows. This is aided by the atmosphere calming chamber, which prevents interference from atmospheric effects. The settings used are shown in Appendix 4. These settings allow for tracking of the majority of particle pairs which was confirmed by experimentation with settings. Attempts to use additional resolution or to allow for higher velocity particles result in little change in steady state flow field results and a substantial increase in convergence time and probability of divergent mappings. Further reading on the technical specifics of this process is available in the Davis manuals [47].

3.4.2 Velocity fields to 3D velocity domain

Such velocity fields can be loaded as multi-dimensional arrays into MATLAB. Using MATLAB, these high dimensional arrays can be combined to get averaged arrays containing the steady-state flow components of each individual data set. This is achieved by taking the root mean square value for each measured dimension at each point in the array. Once these averaged arrays are generated, polynomial interpolation is used along the out-of-plane axis across the various slices of data to produce a flow field in three dimensions. These flow fields can then be mapped and examined for specific flow components, as is discussed in the conclusions section.

Figure 3-18 shows the measured speed fields measured during one experimental regime for the case of a one hundred percent duty cycle in the x direction. Each surface is a measured speed field. All speeds over 0.1m/s are shown, and the colour

denotes the measured speed. Note the axes are not equal, and the y-axis is expanded by a factor of five in order to make the figure more easily readable.

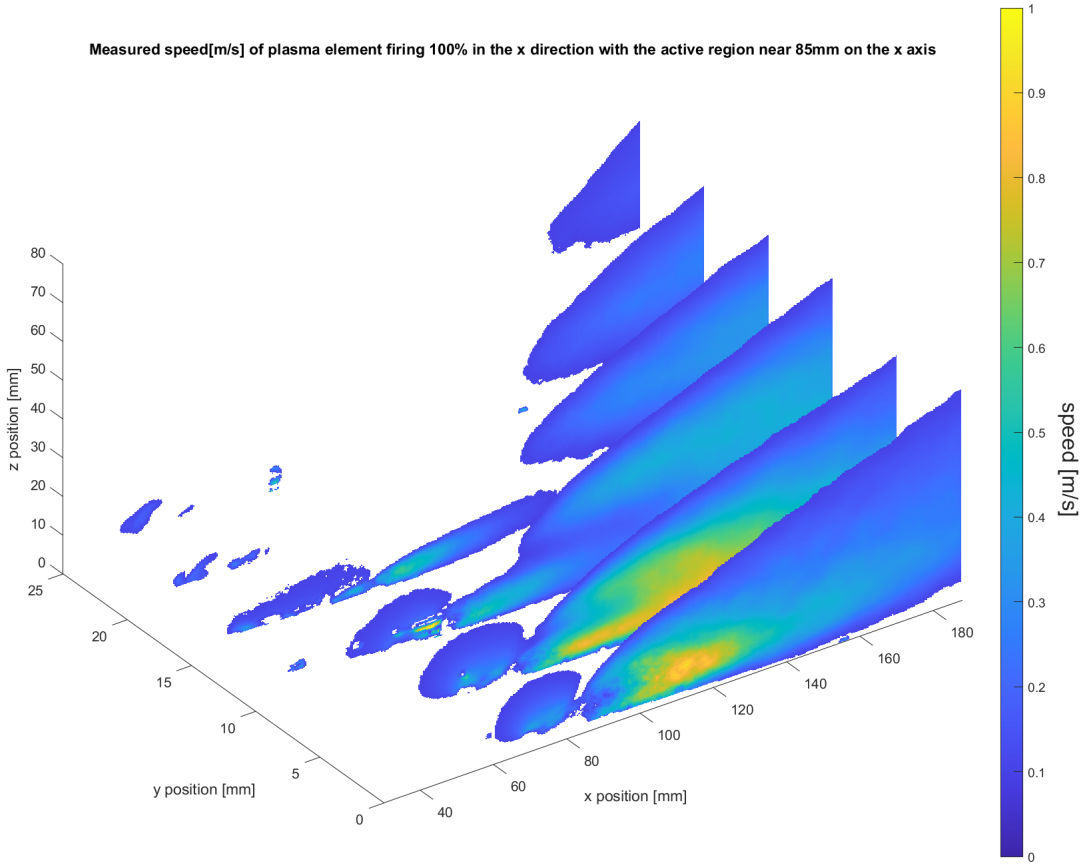

Figure 3-18 Measured speed fields demonstrate location of measured data fields prior to interpolation

.

3.5 Error analysis

3.5.1 Model limitations

Each plasma actuator is hand-constructed; while great care is taken to ensure all dimensions are correct and equal, some dimensions, such as exposed-encapsulated electrode gaps, are extremely sensitive to construction deficiencies. This can result in different relative power between directions in a given plasma element. To correct

for this, the plasma elements were designed to be large (>20mm) so that construction errors in gap distance can be averaged over a longer interface.

Additionally, models must be covered by a non-reflective surface to ensure safety when using the PIV laser. This covering is not completely uniform as some elements must be exposed (top of the encapsulated electrodes and edge of the exposed electrode). While the coating is thin, it has a significantly different surface texture than the underlying Kapton and presents edges where material sheets had to be cut to cover appropriate hardware. These introduce uneven drag effects, which can impact the boundary layer thickness unevenly across the device.

Finally, this study explores proof of concept tests to demonstrate control over such a device and the flow above it and, as such, takes place in quiescent air. This changes the boundary layer properties of the device and affects the domain in which the primary effects are taking place. In quiescent air, plumes of flow induced by the plasma elements and arrays are observed, which depart from the boundary layer and form in the fluid above the test apparatus. In high-subsonic flow domains such as real airframes are likely to encounter plasma actuators primarily act on the boundary layer. Despite this, for the sake of studying the general controllability of such a device, quiescent air will suffice as it is indicative of the directionality of induced flows.

3.5.2 PIV limitations

Due to the brightness of the laser sheet and interference from the visible plasma, there are some regions where particle mapping is not possible. Significantly the region, including the area directly over the interface between the encapsulated and

exposed electrodes, is typically too brightly lit by the plasma and exposed copper components to be accurately imaged for PIV purposes, which prevents detailed examination of this domain. While for the purpose of demonstrating the capacity of this device to drive flow differentially, it is sufficient to study the entrained flow downstream of the interface. There is a limitation to the degree of precision that it is possible to attain when studying the region near the interface.

Additionally, due to the nature of the PIV system, flows out of the plane of the laser sheet are not captured. When studying these flows, best efforts are made to ensure the captured planes contain the relevant flows, including the flow components of concern; however, it is only possible to infer the flow out of the plane qualitatively by examining the flow fields produced and the in-plane flow vectors. This limits the claims that can be made when discussing flow attributes quantitatively to only discussing flows within the plane of the laser sheets.

3.5.3 Polynomial interpolation and uncertainty due to data manipulation

When producing renderings of flow fields, it is necessary to interpolate these fields in the out-of-plane axis. These interpolations, while qualitatively sufficient, introduce a defect proportional to the degree of the polynomial. As such, these interpolated values cannot be used when graphing flow components. Instead, for quantitative measurements, only measured data points are used and no interpolated ones. Figure 3-19 shows the interpolation of the flow fields shown above. Note that the axes in this interpolated field match those of Figure 3-18 and, as such, are not to scale.

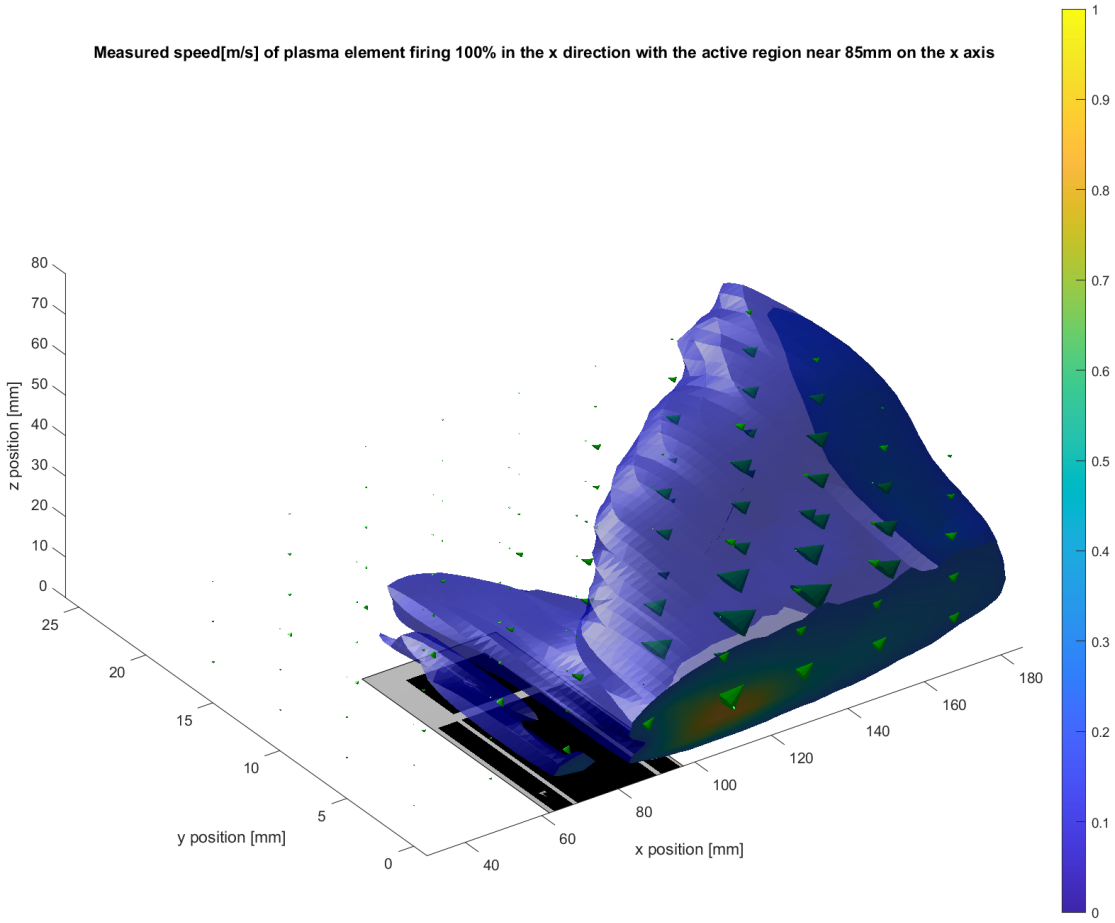

Figure 3-19 The interpolation of the field shown in Figure 3-18 as slices of measured data. Iso-surface showing 0.25m/s.

Chapter 4. Results and Discussion

4.1 Proof of Concept: control of flows coaxial to primary apparatus axes

The most basic requirement of this research is the establishment of a device which can be programmed to produce a system that induces flow in multiple directions with control over which direction is induced within a single geometry. To establish this, the simplest of the test regimes connected only one encapsulated electrode in a four directional plasma element (test geometry 1). Figure 4-1 is an image showing the operation of the device during a test fire before being added to the PIV

apparatus. The visual plasma makes it easy to see initial evidence of differential firing between the encapsulated electrodes within one plasma element. Figure 4-1.a shows the orientation of the plasma element. Figure 4-1.b, shows one directional firing of the plasma element and Figure 4-1.c, shows the apparatus firing in two adjacent directions, both at one hundred percent duty cycles.

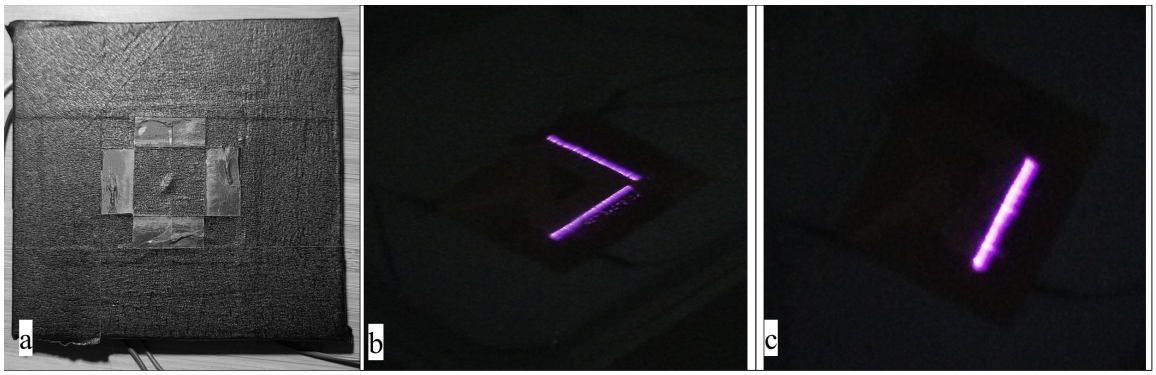

*Figure 4-1 (**a**) A four directional plasma element. (**b** … firing in two adjacent directions. (**c**) …firing in one direction.*

More quantitative evidence is shown in Figure 4-2; the PIV result is shown below. The iso-surface represents 0.1m/s, while the cone plot shows directionality, and the heat map shows a slice of the speed along the primary axis.

This render is qualitative evidence that the device is able to differentially induce flow in the primary axes of the device. By having the positive-direction x-axis encapsulated electrode complete the ac circuit while all other encapsulated electrodes are floating ground, this is able demonstrates that isolation of flow directionality within one geometry and apparatus is possible.

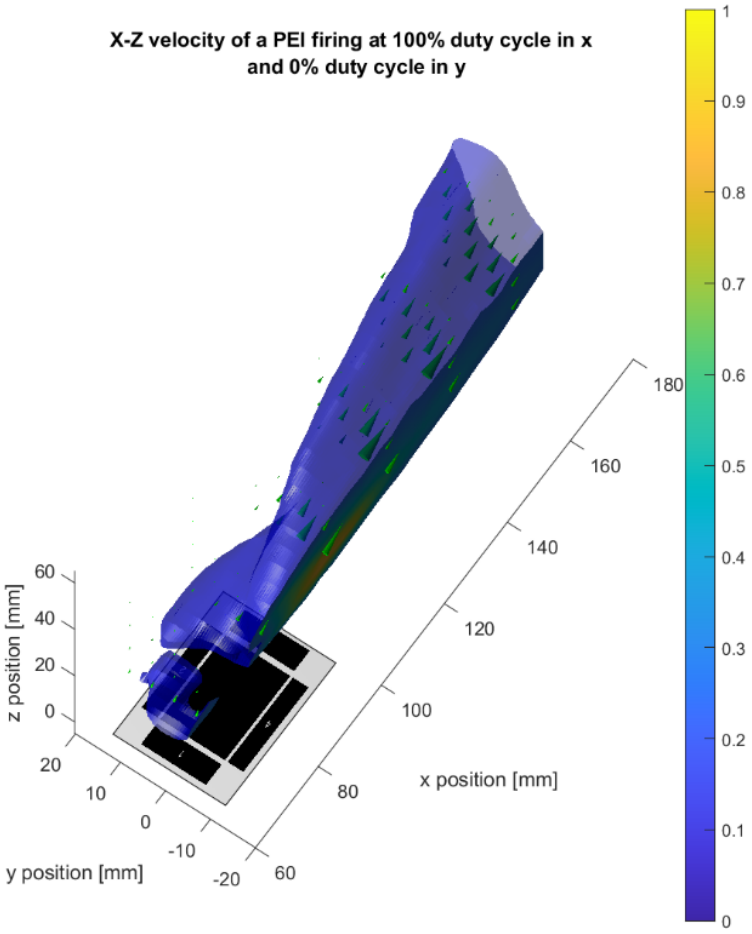

Figure 4-2 A 3D render of xz velocity field above the plane of a plasma element firing 100% in the x direction. Iso-surface shows flow speed equaling 0.25m/s cone plot shows directionality and speed. The heat map on y=0 plane shows speed of flow in the xz plane.

In order to provide additional support for the claim that flow directional isolation has been achieved, xy-plane slices were imaged using the same apparatus. The analysis of this data yields flows calculated at a variety of heights above the test bed. Figure 4-3 shows a variety of slices of the xy-velocity field at heights above the plane, as demarked in the diagram, over a plasma element centered at approximately 14mm on the z axis, 0mm on the y axis, and 100mm on the x axis.

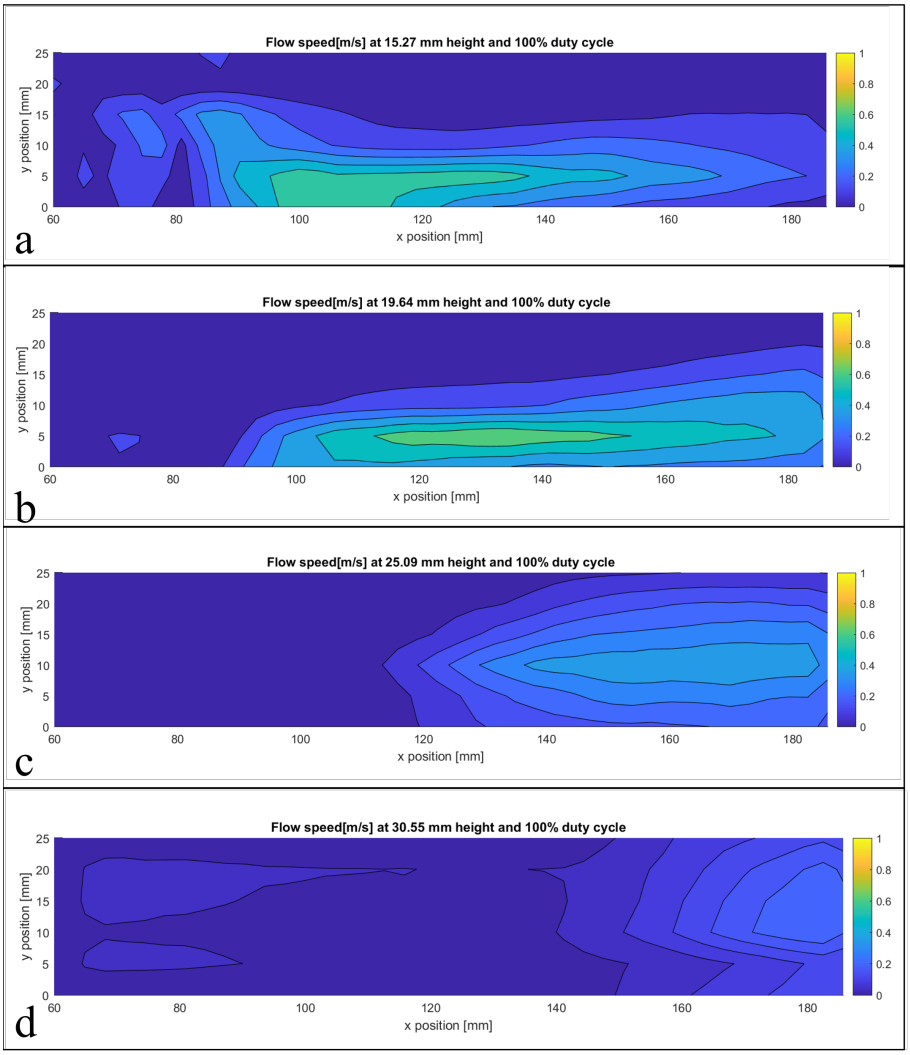

Figure 4-3 x-y flow at various heights above a plasma element firing at one hundred percent in the x direction.

Note the isolation of flow to the X direction. These topological graphs show the speed of the flow in meters per second. Note the induced flow field downstream from the plasma element and the signs of what appears to be flow entrainment immediately upstream of the active region located near 80 mm in the x axis.

In order to ensure that the flows observed are due to the electromotive force induced by the plasma actuator and not due to thermal flow induced by heating of the apparatus these tests were conducted with the apparatus mounted vertically.

The direction of action is horizontal and as such thermal flows would appear as flow in the positive y-direction. As can be seen here there is no significant flow in the y direction. While some small amount of flow in the y axis may be attributed to thermal flow it is readily apparent from the results outlined in figure 4-3 that the primary directionality of flow is in the x axis. This is horizontal in the test apparatus and as such cannot be due to thermal effects.

4.2 Control of arbitrary flows in the plane

Making further use of the first test configuration, it is possible to demonstrate control of the speed of induced flows in the x-direction by varying duty cycles. This establishes not only binary control over the direction of flow but the ability to tune the speed of the flow in each direction differentially. This is critical to the establishment of directional control within the plane.

Figure 4-4 shows the induced speed in the x-axis as a function of the duty cycle in a plasma element firing one encapsulated electrode in the positive x direction.

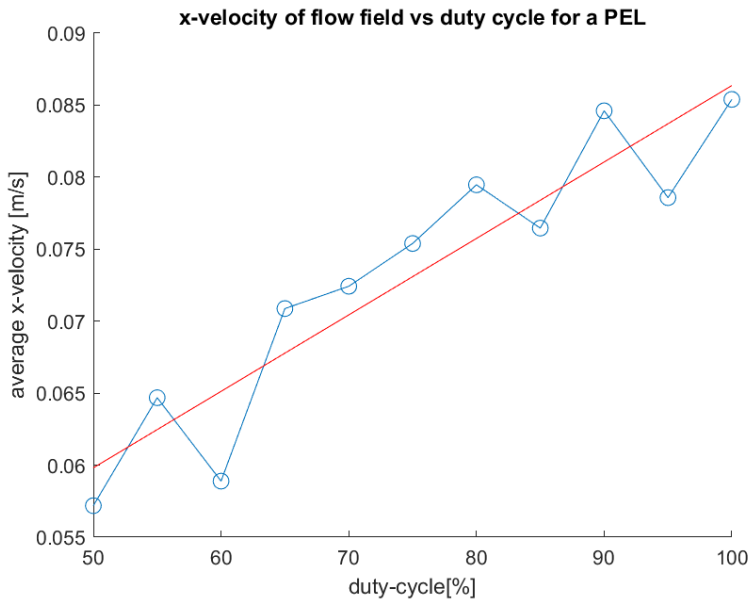

Figure 4-4 A graph of x-velocity vs duty-cycle percentage in a plasma element firing in the positive x direction. Best fit line shows a slope of 2mm/s/%dc with R^2=0.72

The linear best fit line shows a relationship between duty-cycle and x-velocity of two millimeters per second per percent duty cycle (2mm/s/%DC) with an R^2 value of 0.72 for duty cycles above 50%. With this result, it is established that control over the velocity of flows in each primary axis of the device is possible.

Knowing that the flow speed can be controlled along each primary axis, the second testing regime studies the control over flow within the plane of the array by utilizing varying duty cycles in adjacent encapsulated electrodes. By configuring differential duty cycles for adjacent encapsulated electrodes within a test geometry, flows are produced where the mean direction of flow is not colinear to the primary axes of the device. Due to limitations in detecting flows out of the plane of the laser sheet, it is left to infer the flow into/out of the plane from the drift in the induced xz

flow fields. That is to say, detecting steady state flow in the xz plane that originates in the y plane near zero and flows into the y-plane implies flow in the y direction.

Figure 4-5 shows interpolated flow fields at several different duty cycles. Figure 4-5.a shows flow directly in the x direction with one hundred percent flow in the x direction and zero percent in the y direction. Note that the flow is measured starting at the middle of the apparatus, and as such, it is reasonable to expect that it would be symmetrical about the plane y = 0. Figure 4-5.b shows flow at seventy five percent in the x direction and twenty-five in the y direction. In this, little flow along the plane y=0 can be observed, suggesting that the observed flow represents the majority of the induced xz flow field. Figure 4-5.c depicts the x and z components of the flow field when the plasma element is firing fifty percent in the x direction and fifty percent in the y direction. Note the significant drift of the iso-surface depicting 0.1m/s flow speed into the y axis in Figure 4-5.b and c. Such a flow profile is not possible in a steady state without a significant y component to the flow field. Additionally, more y-axis drift is observed in Figure 4-5.c than in Figure 4-5.b, which confirms that by varying the duty cycles of adjacent encapsulated elements, it is possible to exert control over the angle of the imparted momentum.

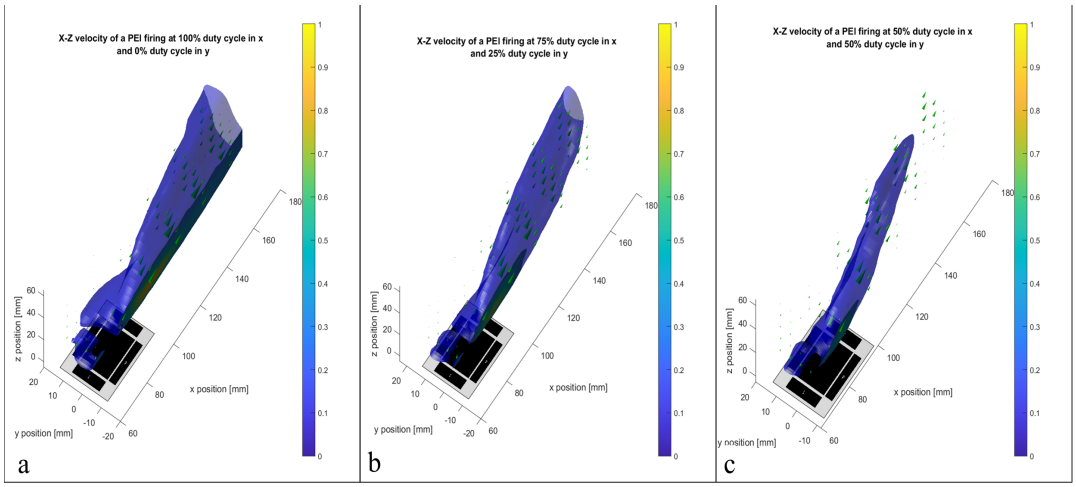

*Figure 4-5 Iso-surface and cone plots representing the x and z components of the flow field induced by a plasma element (shown) firing at: **(a)** 100%x, **(b)** 75%x-25%y, **(c)** 50%x-50%y. Iso-surface at 0.25m/s cones show direction and speed(size)*

Plasma elements are constructed to be symmetrical in each of the primary axes of the device. In this apparatus, this means it is reasonable to expect flows to have no preferential primary axis and to be induced equivalently in each direction. As such, it is reasonable to expect that the observed results should be mirrored in the yz-plane. This can be used to characterize the overall performance of the device in the plane. Taking this into consideration, one notable result is that at a fifty percent duty cycle, the xz flow is not shown to be at forty-five degrees to the primary axes of the device. This shows that there is diffusion of the flow when firing in multiple directions. The quantification of this diffusion is not within the scope of this research but can potentially affect the performance of arrays of plasma elements.

Figure 4-6 depicts top-down views of the same xz flow fields as topological slices showing flow speeds. These results further highlight the flow divergence into the positive y direction as the plasma element is configured to fire more into the y direction. Note that the one hundred percent figure is only depicting flow beginning

halfway across the active region and that the flow field, therefore, will be mirrored across the y=0 axis in Figure 4-6.a. This is not depicted, and although this can safely be inferred from the geometry of the tests, it was not measured directly. Figure 4-6.b and 4-6.c show flow fields which diverge significantly from the y=0 line and therefore are not expected to be symmetrical.

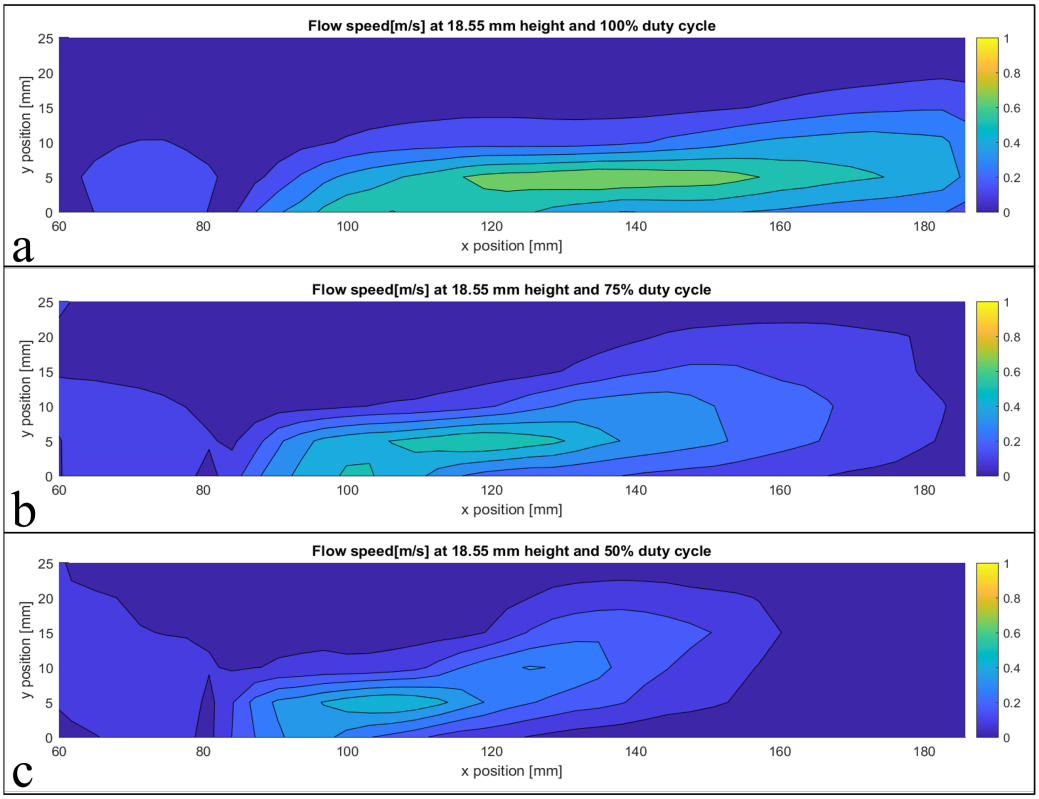

*Figure 4-6 xz flow speed fields at 18.55mm above the test bed zero point (roughly 4.5mm above the testbed) showing flow at: (**a**)100%, (**b**) 75% and (**c**) 50% into the x direction with reciprocal duty cycles in the y-direction.*

These results demonstrate control over flow within one quarter of the plane within the domain of fifty to one hundred percent duty cycles. These results provide the evidence necessary to claim control over the direction of the mean flow induced by the plasma element within the plane in which it is positioned. While there is

significant flow dispersion at a duty cycle of 50%x-50%y the mean flow is still expected to be off axis. Further, the drift of the mean xz flow field into the y axis demonstrates that this flow is not only divergent (flow in x & y respectively) but is actually significantly flowing in a non-coaxial direction.

4.3 Control of flows out of the plane

In order to claim full directional control over flows near the surface and to recreate the flows used in the research reported by Borghi, et al. [7], it is necessary to establish control over jets out of the plane of the apparatus. To this end, test geometry 3 is tested with two sets of two plasma elements (shown in Figure 3-13) firing toward each other with varying duty cycles.

Figure 4-7 demonstrates the effect of varying the duty cycle in the opposing encapsulated electrodes. Initially, both sets of plasma elements fire toward each other at equal duty cycles. This closely replicates the single jet testing performed by Broghi et Al. [6] while making use of our geometry and switching controls.

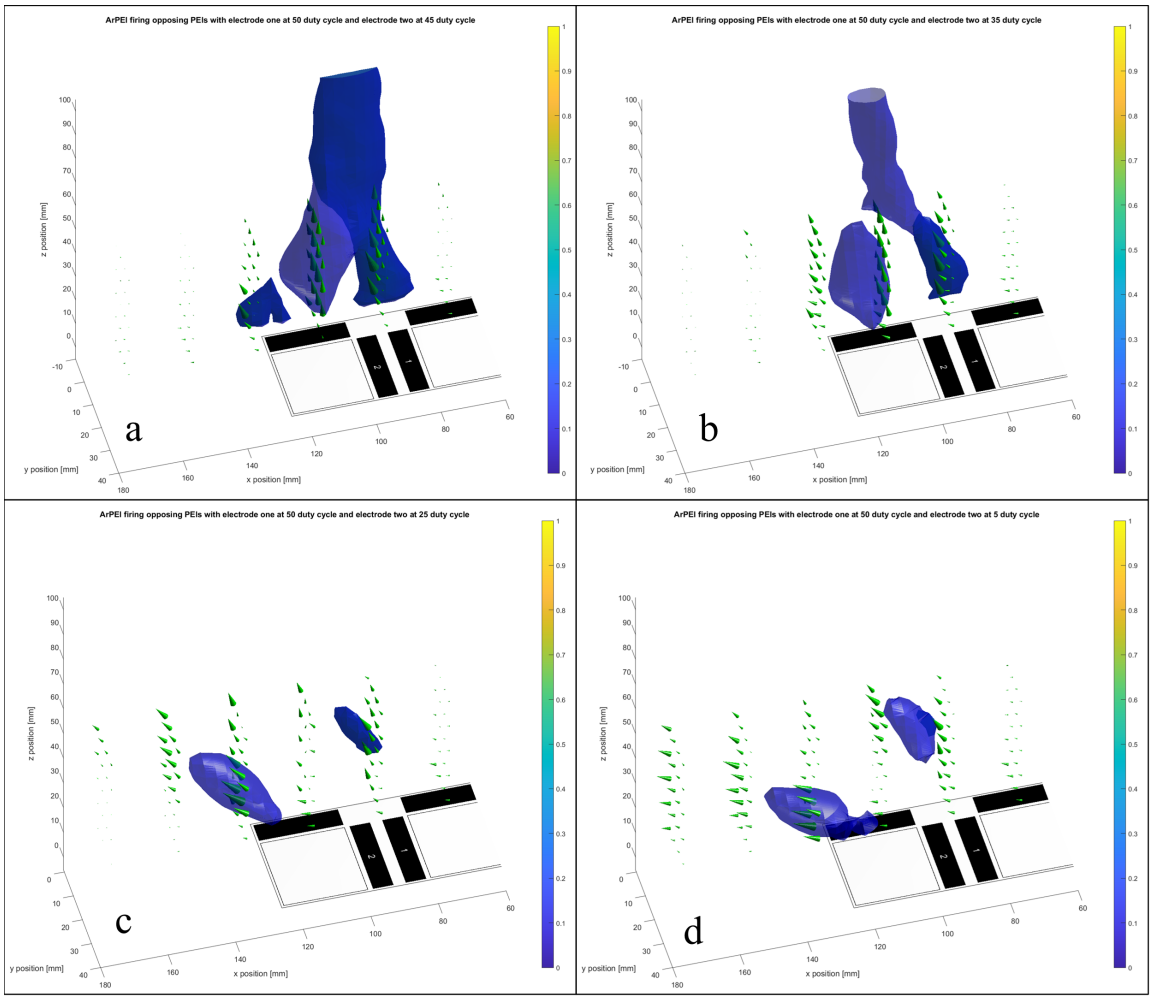

*Figure 4-7 A pair of plasma elements firing towards each other with varying duty cycles. The right-hand electrode (1) is held at 50% duty cycle while the variable electrode (2) is varied. Figure duty cycles are: **(a)** 50-45, **(b)** 50*

As Figure 4-7 shows, it is possible to induce flow out of the plane by firing two plasma elements toward each other such that the flows induced by each are opposing. For these experiments, one plasma element is consistently fired at 50% duty cycle while the other is varied. These flows interact between the plasma elements and induce a net flow away from the surface of the array near the boundary between the plasma elements. This flow can be observed clearly in the cone plots of Figure 4-7 as well as in the 0.25m/s iso-surface.

Figure 4-8 shows topo graphs showing flow speeds for varying duty cycles.

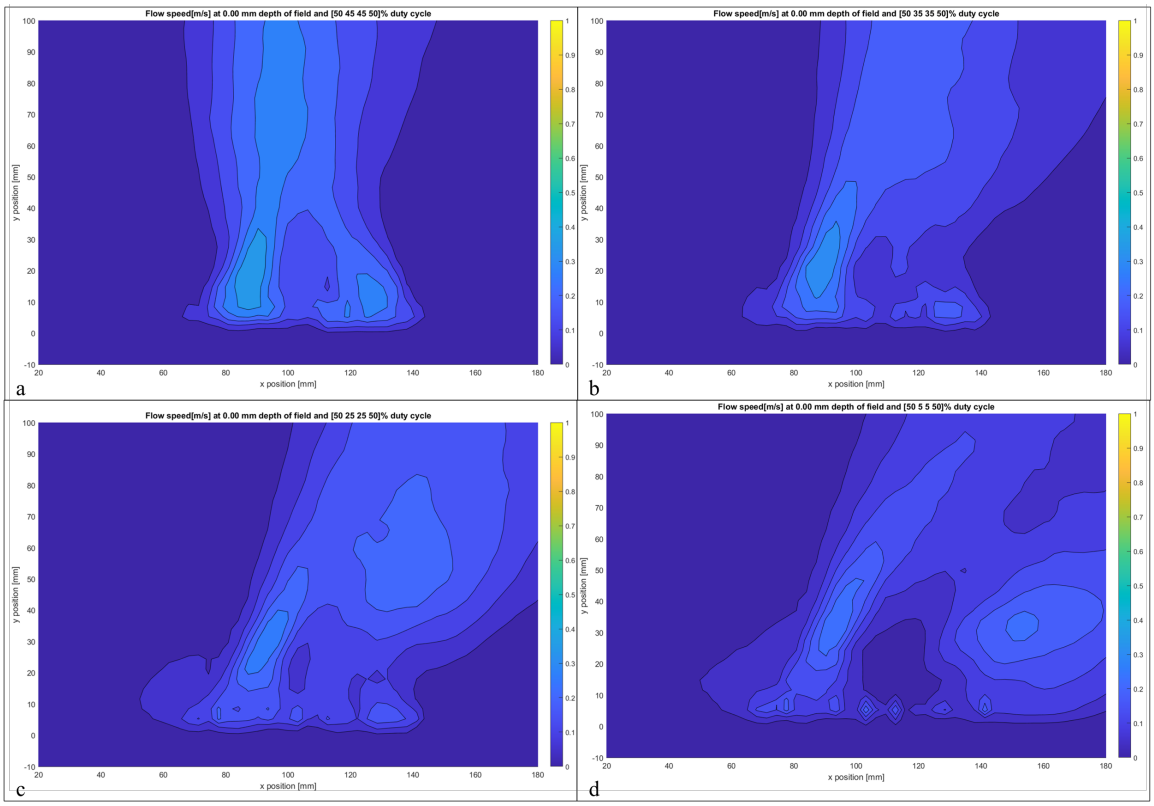

Figure 4-8 Topographical graphs of flow speed for flows induced by two opposing plasma elements actuating towards each other. The interface between the two elements is at approximately 100 in the x-axis with the activation regions near 80 and 120. The left-hand actuates at 50% for all tests while the right-hand actuator actuates at successively lower duty cycles. a.=50%-45%, b = 50%-35%, c = 50%-25%, d = 50%-5%

These results show not only that can such an apparatus produce jets out of the plane, analogous to those used in the research reported by Broghi et al.[7], but by varying the duty cycle of the opposing plasma elements, it is possible to affect control over the mean azimuthal angle of the flow induced out of the plane of the array. Figure 4-9 also shows the relationship between the azimuthal angle and the duty cycles.

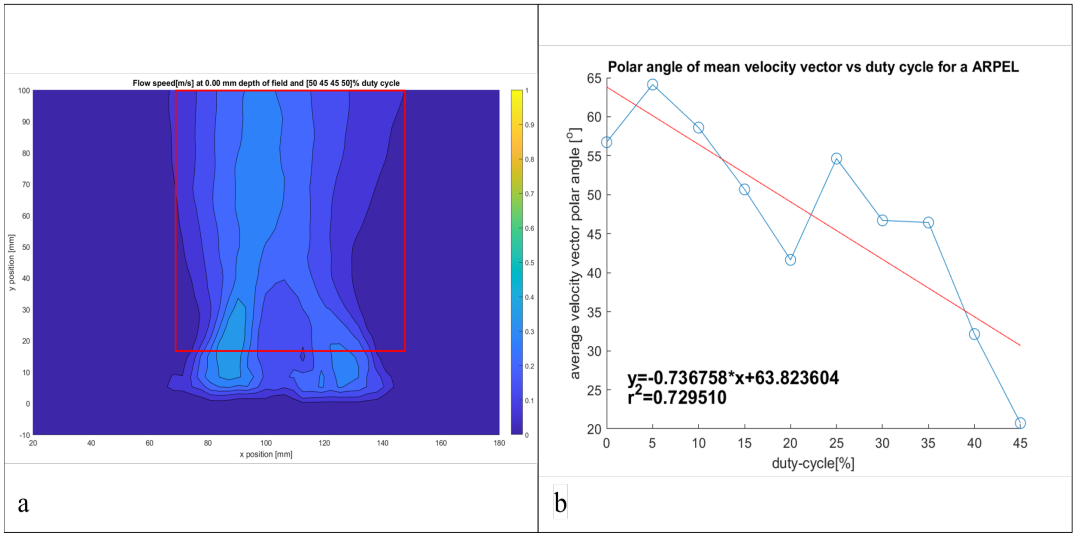

Figure 4-9 Azimuthal angle of mean induced velocity field as a function of duty cycle in the variable plasma element.

These results allow us to further characterize the flows induced at a variety of duty cycles in the variable plasma element in such a configuration. Figure 4-10, below, demonstrates the average speed, x-axis velocity and z-axis velocity at varying duty cycles. A clear positive correlation exists between the duty cycle and the overall speed of the flow, which is as expected since this higher duty cycle provides more time for the plasma elements to induce momentum. The z-velocity increases as duty cycles equalize, likely due to the increased energy and velocity of the induced flows, which translate into higher z-axis flow rates when the flows interact. Finally, the average x-axis velocities approach zero as duty cycles equalize, which further supports the claim that these devices should behave equally regardless of the direction of actuation.

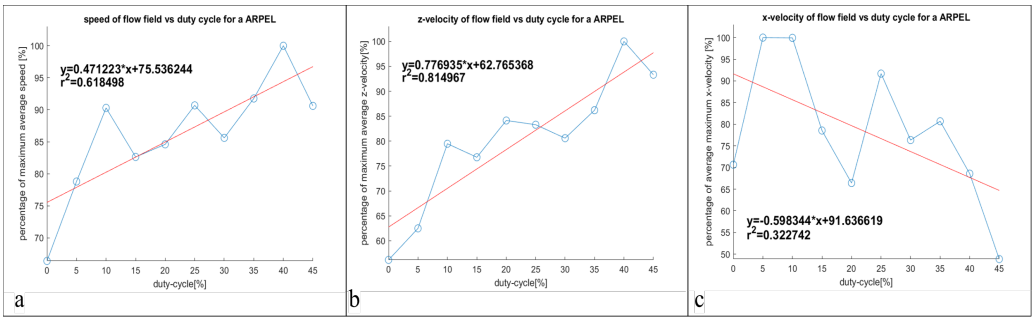

*Figure 4-10 Average flow speed (**a**) x(**b**) and z (**c**) components of velocity at a variety of duty cycles within the variable plasma element in plasma configuration three*

4.4 Production of non-normal, non-coaxial, flows out of the plane

As a final proof that this apparatus is able to produce truly arbitrary flow directions out of the plane, plasma configuration three is wired to allow individual control over each plasma element so as to produce a flow that is not coaxial to any geometry in the plasma element and is not fully normal to the plane of the apparatus either. Such flow demonstrates the ability of such an array of plasma elements to produce flows that are decoupled from the underlying geometry of the array.

For the purpose of these tests, each plasma element is wired to fire both adjacent, inward-facing, actuators at the same duty cycle. The four half-plasma elements described in Figure 3-17 are then fired, with each plasma element actuating at different duty cycles. While finer grain flow control is likely possible by differentially actuating each encapsulated electrode within each plasma element, characterization of such control is beyond the scope of this research.

Figure 4-11 demonstrates the flows described above. These renderings lack the y-axis flow due to imaging constraints, however, it is possible to observe flows which

vary greatly when differential duty cycles are applied to each of the four plasma elements. Each unique configuration of the duty cycle produces unique flows. The upward flow predominantly near the plane at x=0 is likely due to the fully captured flow induced by the opposing y-axis encapsulated elements. There may be a thermal component; however, the highly varied velocity of the central jet, along with the differential upstream paths of the flow, as shown by the streamlines, suggest that these are controlled jets which are varied by the duty cycle of the underlying plasma element.

While this experimentation does not provide enough data to quantitatively define the relationship between the varying of the four duty cycles and the generated flow regimes, the variance shown does demonstrate that flows, not normal to the surface, may be produced. Given that the system is symmetrical in the x and y axes, it is reasonable to conclude that such effects are present in the y-axis and that directional flow control is occurring based on the varying duty cycles.

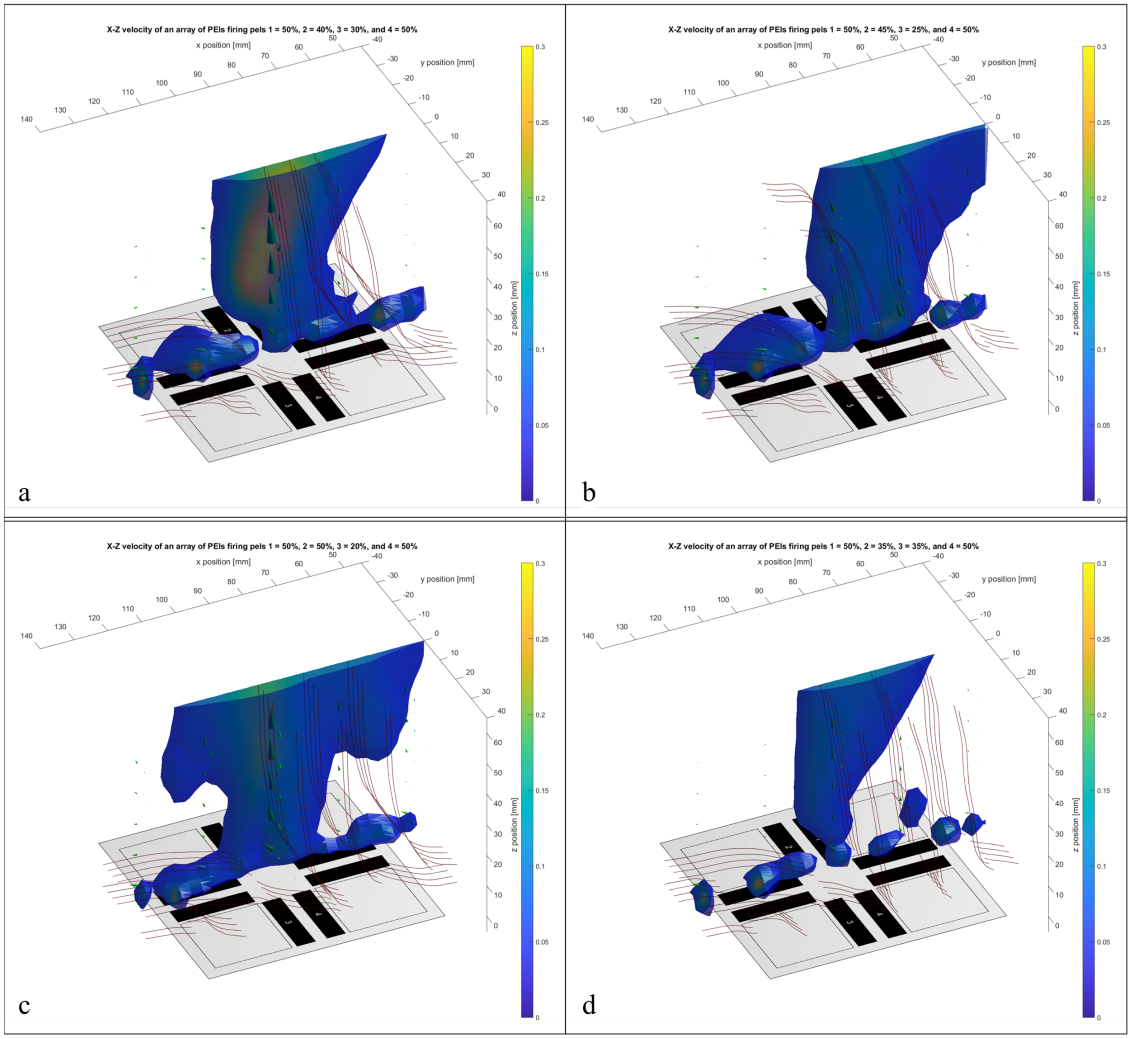

Figure 4-11 Flows generated via varied duty cycles. These demonstrate the ability to vary flow profiles through differential actuation of plasma elements.

4.5 Summary of Results

The qualitative results shown in Figure 4-1 are a clear indicator that the device is able to actuate its encapsulated electrodes differentially. The light given off by the plasma provides a simple and convenient way to observe the differing intensity of actuation when two adjacent actuators are firing versus when only one is firing. While this qualitative evidence is helpful, the evidence shown in Figures 4-2 and 4-3 provides quantification to these claims. The flow field clearly shows induced

flows originating at the active interface of the firing encapsulated electrode within the plasma element under test. With this verified and keeping in mind the symmetry of the underlying apparatus, it is reasonable to claim the ability to generate flows which can be programmed to proceed along any of the primary axes of a plasma element.

This result is novel as one can now produce flows with programmable directionality without varying the physical construction of the plasma element (plasma actuators). In the interest of re-creating the desired flows locally at a given point in the array, it is sufficient to produce flows which are coaxial to the primary axes of the device as well as flows normal to the surface of the wing. With the demonstrated ability to produce these basic flows, this research should provide sufficient evidence that these arrays can be used to recreate the desired induced flows and as such, may form the basis for more flexible and responsive flow control systems.

In the interest of exploring the full space of flow directionality that such a device can produce, adjacent encapsulated elements were actuated at varying duty cycles. The results in Figures 4-5 and 4-6 show qualitative evidence of flow progressing not only in the x-direction but in the y-direction as well. While there are limitations to the dataset which limit the ability to infer the y-axis flow, it is reasonable to state that some y-axis flow is induced in the mean flow due to the presence of y-axis drift in the isosurface of the xz-velocity in Figure 3-18 and the corresponding evidence in the topographical graph in Figure 4-6. This divergence is not symmetrical about the plane y=0, as can be seen by the lower flow speeds on that

plane and the jet-like appearance of the isoplane. As these figures show time-averaged flows, these results are not possible without some y-axis component to the flow. This aligns with the expectation of mean flow induction in a direction that is not co-linear to the primary axes of the device.

Figure 4-4 further supports these claims as it shows the x-axis velocity varying with the duty cycle. A linear fit has an equation of:

Equation 4-1 linear fit of x-velocity as a function of duty cycle

$$speed = (0.621710 * \text{duty\_cycle} + 38.95574) * maximum\_speed$$

in the range where duty cycle has value between 50 and 100 percent with an R^2 value of approximately 0.86. Knowing that a duty cycle of zero percent should produce zero induced momentum, it becomes apparent that there is non-linearity in the relationship between the duty cycle and the induced flow speed somewhere outside of this range of duty cycles. However, in the explored domain of duty cycles, the evidence shows that the induced flow varies linearly with the changes in the duty cycle. Since the device is symmetrical on the x and y axes, this provides evidence that this device is able to produce mean flows which are not colinear to the primary axes of the device. Quantifying the dispersion of these flows is beyond the scope of this work; however, qualitatively, it appears that there is non-linear interaction between these flows resulting in less dispersion than would be expected from the non-interacting addition of these flows. This is suggested by the results mentioned in the prior paragraph, where the isoplane representing the induced flows drifts into the y-axis. Such behaviour can be explained due to momentum from the upstream flow being entrained by the device. That is to say, as the y-axis

encapsulated electrode fires, it entrains flow with y-axis momentum. Some of this flow is actuated by the x-axis encapsulated electrode, which adds x-axis momentum to the flow without removing the y-axis momentum the flow already contained. Thus, while the flow progresses down, the x-axis also progresses down the y-axis, which is observed by these experiments. There are likely other turbulent and non-adiabatic forces involved, however, these are beyond qualitative assessment given the current dataset.

These qualitative and quantitative results support the claim that such a device is able to produce flows with any given mean direction within the plane of the array. As the flow modification in points 1, 2, and 3 are all generated through flow modifications that are within the plane of the plasma actuator(s) generating them, these results establish that the plasma element is able to produce them.

Having demonstrated that such devices are able to generate mean flows at arbitrary directions within the plane, it is left to produce flows out of the plane. The results demonstrated in Figures 4-7 and 4-8 provide qualitative support for the claim that two opposing plasma elements, arranged within a regular array of plasma elements, are able to produce flows not only normal to the plane of the array but with controllable polar angles. Figure 4-9 shows the relationship between the opposing duty cycles and the achieved polar angle in the region above the active plasma elements. The slope of the graph is 0.75 degrees of polar angle per percentage of variable duty cycle encapsulated electrode. While there appears to be higher order phenomenon at play, reducing the R^2 value to approximately 0.72, a clear trend is observable correlating the value of the opposing duty cycles and the induced

momentum flow. This correlation is unambiguous evidence that the array being tested is able to induce flow out of the plane with polar angles in the range of 55 to 20 degrees. Knowing that the arrays exhibit a mirror symmetry across the interface between two plasma elements and examining the final three data points in the range, which have an average slope of ~2.7 degrees of polar angle per percentage duty cycle, the data suggests that at matching opposing duty cycles the flow should be within 8 degrees of the vertical axis. Since the array exhibits no geometrical or electrical preference in direction, this provides evidence that such an array is able to produce flows with polar angles less than approximately 65 degrees.

The final test is qualitative in nature. It stands to reason that since such arrays are able to induce flows at polar angles other than 0 degrees and since the arrays exhibit radial symmetry, it should be possible to induce flows out of the plane of the array at arbitrary polar and radial angles. In order to produce qualitative evidence of such flows, a variety of test regimes were explored in which four plasma elements fire at differing duty cycles. The results obtained are shown in Figure 4-11. These datasets do not contain the y-axis components of the flow; however, it is apparent that significantly different flows are induced by the different duty cycles. Notably, the streamline directions and loci of high-speed flows vary with changes to y-axis duty cycles. This suggests that significant flow modifications are being produced by these changes. Further, the flow regimes exhibit differentiated directionality when compared qualitatively to the flows studied in the ArPEl tests, as shown in Figure 4-7. This implies that these flows are distinct when compared to the flows induced colinear to the x-axis. This forms

qualitative evidence that such arrays are able to induce flows that are not entirely constrained to be colinear to any primary axis of the array.

Chapter 5. Conclusion and Recommendations

5.1 Conclusions

The central purpose of this research is the demonstration of a programmable Plasma Element capable of generating directionally differentiated flows without underlying changes to the physical construction of the device. This goal was set with the purpose of reproducing five flows demonstrated to generate useful modifications to the behaviour of airframes. The aim was not only to re-create these induced flow regimes but to characterize the space of flows such a device is able to generate. Firstly, to demonstrate control over directional firing within the proposed device by actuating only one encapsulated electrode. Secondly, control within the plane of the array using varying duty cycles of adjacent encapsulated electrodes. Thirdly, establishing flow production out of the plane of the array using opposing plasma elements within an array. Finally, to demonstrate that flow which is non-coaxial to any geometry of the device, is likely being generated from the array.

The primary contribution of this work is the establishment of a directionally programmable dielectric barrier discharge plasma actuator (a plasma element) and arrays of these plasma elements (ArPEls). This research has demonstrated that these plasma elements are able to induce flow in a variety of directions within the

plane of the plasma element, including directions that are not coaxial to any of the primary axes of the devices. Further, this research has shown that arrays of these plasma elements are able to induce flow with mean direction out of the plane of the array and that it is possible to exert control over the polar and radial angles. This research presents an initial survey of the flow directionality such arrays are able to generate and establishes that these flows are sufficient to reproduce 5 useful flow modifications previously established as being beneficial in the control of airframes.

By establishing these results, which demonstrate control over induced mean flow direction out of the array at polar angles below 65 degrees as well as control over mean flow direction within the plane of the array, this research has established that a regular array of plasma elements is able to produce a superset of the flows required to re-create the listed beneficial flow modifications. That is, the space of flows required to induce these individually beneficial modifications to lift body performance is a subset of the space of flows which can be produced by this array. Further, as the plasma element can be programmed to produce each of the desired flows with no physical modification to their geometry or electrical configuration, this has demonstrated the ability to vary the production of these flows over time. Finally, as each plasma element is identical, there are no preferential locations within the interior of the array, and therefore each modification can be generated at any plasma element fully within the array. This demonstrates that an ArPEl is able to produce flows with a programmable direction near the surface of the array.

5.2 Contribution and Novelty

During the course of this research a novel design of plasma actuator is tested for the ability to produce directionally controlled thrust within the plane of the array. Further, arrays of such devices are used to produce flows out of the plane and to demonstrate the ability to control said flows directionally. By making use of computer controlled high voltage switching arrays it is possible to modify duty cycles of the various encapsulated electrodes and to produce flows that are directionally differentiated based on these varied duty cycles. This geometry of plasma actuator is novel within the literature and has not been seen before. Further devices utilizing high voltage switching for directional control of flows within an array are not currently present in the literature.

This gap in literature is likely due to present research focusing largely on the ability to improve performance of plasma actuators, both in thrust generating capacity and in efficiency. Most research into plasma actuators at present appears to focus on either the mechanisms of plasma generation, and modeling, or on the ability to produce novel flows as a result of the use of plasma actuators. In opposition to this the devices studied herein do not produce any new effects that have not been produced elsewhere in literature. Instead, they provide a methodology for generating the flows required for these effects without requiring specialized geometries.

The merit of these novel plasma actuator apparatus (plasma elements and arrays thereof) is in the ability to produce a variety of flows at a variety of locations within the array without bias as to location or time. That is to say, the studied arrays are

able to produce flows which can be programmatically which in the past required specialized actuator geometries to induce. This ability allows an operator to define, at the time of use, which effects they require from the plasma actuator array and where they require them. Such an array of devices can for a generic substrate which can induce a wide variety of effects by programming them into the computer controlling the switching array. These effects can vary in time and space and are agnostic to the location or time they are required to present within the array.

The benefit of a regular array of directionally programmable plasma actuators is to allow for programmable flow fields near the surface of the array. The ability to select desired flow directionality at a given location and time forms the basis for the use of such arrays to control airframes, reduce noise, and modify flight parameters for aircraft and lifting bodies. By recreating flows with known effect on airframes this research provides a proof of concept for the use of such arrays of programmable multi directional plasma actuators to: 1. Improve performance of lifting bodies by reducing drag. 2. Reduce vibrations by modifying entrainment and vortex generation differentially across a wing encountering turbulence. 3.Reduce structural complexity in wings by reducing tip vortices and the associated complexity of construction. 4. Act as a safety feature by re-entraining detached flows. And 5. by forming the basis for flight control without the use of actuating surfaces by modifying the coefficients of lift and drag differentially across an airframe.

5.3 Recommendations for Future Work

This research forms the basis of the claim that an array of programmable multi-directional dielectric barrier discharge plasma actuators, or ArPEl for short, is able

to produce a space of induced flow directions which is a superset of the flows required for several beneficial modifications to lifting body performance. The research focuses on the design of the array and quantitative and qualitative characterization of the directional control over the mean flows induced in order to support the claim. There are several useful extensions to this research which are now ready to be explored. Firstly, further exploration of the induced flows, including quantification of the dispersion of off-axis flows, the degree to which re-entrainment can be utilized by such an array, the effects of interaction between elements in the array, and the degree to which each effect can be localized within an array, and the performance of such an array in non-quiescent environments. Secondly, exploration of the dynamic performance of such arrays, specifically the definition of the settling time for such a system as the required outputs vary in time. Finally, the further exploration of using solid state high voltage switching such as IGBTs to reduce the cost and weight of the electrical control systems for these arrays. With these domains further explored, it should be possible to run tests using these arrays to modify the behaviour of airframes or even to evaluate these as control systems for aircraft.

Bibliography

[1] Francis Hauksbee, Physico-mechanical Experiments on Various Subjects: Containing an Account of Several Surprizing Phaenomena Touching Light and Electricity, Producible on the Attrition of Bodies. With Many Other Remarkable Appearances, Not Before Observ'd. Together with the Explanations of All the Machines,(the Figures of which are Curiously Engrav'd on Copper) and Other Apparatus Us'd in Making the Experiments. R. Brugis, 1709. Accessed: Jan. 07, 2023. [Online]. Available: https://books.google.ca/books?id=APxlAAAAcAAJ&printsec=frontcover&source=gbs_ge_summary_r&cad=0#v=onepage&q&f=false

[2] Seversky Alexander P De, "Electrostatic ion thrusters characterised by the acceleration grid," US3130945A, Aug. 31, 1959

[3] T. Corke, E. Jumper, M. Post, D. Orlov, and T. McLaughlin, "Application of weakly-ionized plasmas as wing flow-control devices," in 40th AIAA Aerospace Sciences Meeting & Exhibit, 2002. Doi: 10.2514/6.2002-350.

[4] J. Roth, D. Sherman, and S. Wilkinson, "Boundary layer flow control with a one atmosphere uniform glow discharge surface plasma," in 36th AIAA Aerospace Sciences Meeting and Exhibit, in Aerospace Sciences Meetings. American Institute of Aeronautics and Astronautics, 1998. Doi: doi:10.2514/6.1998-328.

[5] M. Tajmar, "Biefeld-Brown Effect: Misinterpretation of Corona Wind Phenomena," Aiaa Journal – AIAA J, vol. 42, pp. 315–318, Jan. 2004, doi: 10.2514/1.9095.

[6] C. A. Borghi, A. Cristofolini, A. Rossetti, G. Neretti, S. Paolo, and A. Talamelli, "Wind Tunnel Experiments on a NACA0015 Airfoil Equipped with Vectorizable Dielectric Barrier Discharge Plasma Actuators," in 32nd AIAA Applied Aerodynamics Conference, doi: 10.2514/6.2014-2684.

[7] C. A. Borghi, A. Cristofolini, G. Neretti, P. Seri, A. Rossetti, and A. Talamelli, "Duty cycle and directional jet effects of a plasma actuator on the flow control around a NACA0015 airfoil," Meccanica, vol. 52, no. 15, pp. 3661–3674, Dec. 2017, doi: 10.1007/s11012-017-0692-3.

[8] P. ~N. Kazanskiy, I. ~A. Moralev, V. ~A. Bityurin, and A. ~V. Efimov, "Active flow control on a NACA 23012 airfoil model by means of magnetohydrodynamic plasma actuator," in Journal of Physics Conference Series, in Journal of Physics Conference Series, vol. 774. Nov. 2016, p. 12153. Doi: 10.1088/1742-6596/774/1/012153.

[9] S. G. Pouryoussefi and M. Mirzaei, "Experimental Study of the Unsteady Actuation Effect on Induced Flow Characteristics in DBD Plasma Actuators," Plasma Science and Technology, vol. 17, no. 5, p. 415, May 2015, doi: 10.1088/1009-0630/17/5/09.

[10] J. Ferry and J. Rovey, “Thrust Measurement of Dielectric Barrier Discharge Plasma Actuators and Power Requirements for Aerodynamic Control,” in 5th Flow Control Conference, doi: 10.2514/6.2010-4982.

[11] M. Sun, B. Yang, Z. T. Zhang, and M. K. Lei, “Experimental study on flow hysteresis effect on NACA0015 airfoil using DBD plasma actuator,” Surf Coat Technol, vol. 228, pp. S179–S183, 2013, doi: https://doi.org/10.1016/j.surfcoat.2012.06.033.

[12] G. Boesch, H. Vo, B. Savard, C. Wanko-Tchatchouang, and N. Mureithi, “Flight Control Using Wing-Tip Plasma Actuation,” J Aircr, vol. 47, pp. 1836–1846, Nov. 2010, doi: 10.2514/1.44003.

[13] M. Han, J. Li, Z. Niu, H. Liang, G. Zhao, and W. Hua, “Aerodynamic performance enhancement of a flying wing using nanosecond pulsed DBD plasma actuator,” Chinese Journal of Aeronautics, vol. 28, no. 2, pp. 377–384, 2015, doi: https://doi.org/10.1016/j.cja.2015.02.006.

[14] T. C. Corke, Design of aircraft. Pearson, 2003.

[15] B. Xue and Y. Yang, “Airfoil leading edge separation flows under control of plasma actuator,” Chinese Journal of Computational Physics, vol. 25, no. 6, pp. 689–693, Nov. 2008.

[16] T. JUKES, T. SEGAWA, S. WALKER, H. FURUTANI, N. IKI, and S. TAKEKAWA, “Active Separation Control over a NACA0024 by DBD Plasma Actuator and FBG Sensor,” Journal of Fluid Science and Technology, vol. 7, no. 1, pp. 39–52, 2012, doi: 10.1299/jfst.7.39.

[17] Dmitry F. Opaits, “Dielectric Barrier Discharge Plasma Actuator for Flow Control,” Princeton, New Jersy, Sep. 2012.

[18] A. Esfahani, A. Singhal, C. J. Clifford, and M. Samimy, “Flow Separation Control over a Boeing Vertol VR-7 using NS-DBD Plasma Actuators,” in 54th AIAA Aerospace Sciences Meeting, doi: 10.2514/6.2016-0843.

[19] X. ZHANG, H. LI, Y. HUANG, K. TANG, and W. WANG, “Leading-edge flow separation control over an airfoil using a symmetrical dielectric barrier discharge plasma actuator,” Chinese Journal of Aeronautics, vol. 32, no. 5, pp. 1190–1203, 2019, doi: https://doi.org/10.1016/j.cja.2019.03.010.

[20] M. P. Patel et al., “Scaling Effects of an Aerodynamic Plasma Actuator,” J Aircr, vol. 45, no. 1, pp. 223–236, 2008, doi: 10.2514/1.31830.

[21] C. He, T. C. Corke, and M. P. Patel, “Plasma Flaps and Slats: An Application of Weakly Ionized Plasma Actuators,” J Aircr, vol. 46, no. 3, pp. 864–873, May 2009, doi: 10.2514/1.38232.

[22] N. Md Daud, Y. Kozato, S. Kikuchi, and S. Imao, "Control of leading edge separation on airfoil using DBD plasma actuator with signal amplitude modulation," J Vis (Tokyo), vol. 19, no. 1, pp. 37–47, 2016, doi: 10.1007/s12650-015-0283-0.

[23] M. K. Phan and J. Shin, "Numerical investigation of aerodynamic flow actuation produced by surface plasma actuator on 2D oscillating airfoil," Chinese Journal of Aeronautics, vol. 29, no. 4, pp. 882–892, 2016.

[24] E. C. Batlle, R. Pereira, M. Kotsonis, and G. de Oliveira, "Airfoil Optimisation for DBD Plasma Actuator in a Wind Energy Environment: Design and Experimental Study," in 55th AIAA Aerospace Sciences Meeting, doi: 10.2514/6.2017-1578.

[25] N. Hall, "Downwash effects on lift," www.grc.nasa.gov, 2015. https://www.grc.nasa.gov/WWW/K-12/airplane/downwash.html. (accessed Jan. 07, 2023).

[26] Karthik Ramakumar and Jamey D. Jacob, "Flow Control And Lift Enhancement Using Plasma Actuators," in 35th Fluid Dynamics Conference, Toronto, ON, Jun. 2005.

[27] T. Mizokami, D. Noguchi, and K. Fukagata, "Lift and drag control using dielectric barrier discharge plasma actuators installed on the wingtips," in 21st AIAA Computational Fluid Dynamics Conference, Reston, Virginia: American Institute of Aeronautics and Astronautics, Jun. 2013. Doi: 10.2514/6.2013-2456.

[28] J. R. Roth, "Aerodynamic flow acceleration using paraelectric and peristaltic electrohydrodynamic effects of a One Atmosphere Uniform Glow Discharge Plasma," Phys Plasmas, vol. 10, no. 5, pp. 2117–2126, Apr. 2003, doi: 10.1063/1.1564823.

[29] J.-J. Wang, K.-S. Choi, L.-H. Feng, T. N. Jukes, and R. D. Whalley, "Recent developments in DBD plasma flow control," Progress in Aerospace Sciences, vol. 62, pp. 52–78, 2013, doi: https://doi.org/10.1016/j.paerosci.2013.05.003.

[30] F. O. Thomas, T. C. Corke, M. Iqbal, A. Kozlov, and D. Schatzman, "Optimization of Dielectric Barrier Discharge Plasma Actuators for Active Aerodynamic Flow Control," AIAA Journal, vol. 47, no. 9, pp. 2169–2178, Sep. 2009, doi: 10.2514/1.41588.

[31] R. Erfani, H. Zare-Behtash, C. Hale, and K. Kontis, "Development of DBD plasma actuators: The double encapsulated electrode," Acta Astronaut, vol. 109, pp. 132–143, 2015.

[32] D. Poon, D. Ernie, U. Kortshagen, and T. Simon, "Experimental studies of plasma actuator performance for separation control," in 48th AIAA Aerospace Sciences Meeting Including the New Horizons Forum and Aerospace Exposition, 2010, p. 1219.

[33] E. Moreau et al., “Surface dielectric barrier discharge plasma actuators,” ERCOFTAC Bulletin, vol. 94, pp. 5–10, 2013.

[34] T. Matsuno, M. Sugahara, H. Kawazoe, and H. Nishida, “Development of serrated multi-electrode plasma actuators for enhanced force production,” in 54th AIAA Aerospace Sciences Meeting, 2016, p. 1691.

[35] T. Corke et al., “Order of Magnitude Improvement of SDBD Actuator Effect,” Notre Dame, Nov. 2006.

[36] S. Sato and N. Ohnishi, “Influence of Voltage Waveform on Electrohydrodynamic Force in a Dielectric-Barrier-Discharge Plasma Actuator,” in 55th AIAA Aerospace Sciences Meeting, doi: 10.2514/6.2017-1804.

[37] M. P. Patel, A. B. Cain, C. C. Nelson, T. C. Corke, and E. H. Matlis, “Shock generation and control using dbd plasma actuators,” 2012.

[38] N. Webb, C. Clifford, and M. Samimy, “Control of oblique shock wave/boundary layer interactions using plasma actuators,” Exp Fluids, vol. 54, no. 6, p. 1545, 2013, doi: 10.1007/s00348-013-1545-z.

[39] Z. Zhao, J.-M. Li, J. Zheng, Y. D. Cui, and B. C. Khoo, “Study of Shock and Induced Flow Dynamics by Nanosecond Dielectric-Barrier-Discharge Plasma Actuators,” AIAA Journal, vol. 53, no. 5, pp. 1336–1348, 2015, doi: 10.2514/1.J053420.

[40] R. Erfani, H. Zare-Behtash, and K. Kontis, “Influence of shock wave propagation on dielectric barrier discharge plasma actuator performance,” J Phys D Appl Phys, vol. 45, no. 22, p. 225201, May 2012, doi: 10.1088/0022-3727/45/22/225201.

[41] Y. Suzen, G. Huang, J. Jacob, and D. Ashpis, “Numerical Simulations of Plasma Based Flow Control Applications,” in 35th AIAA Fluid Dynamics Conference and Exhibit, doi: 10.2514/6.2005-4633.

[42] “8-bit Microcontroller with 8/16/32K Bytes of ISP Flash and USB Controller,” no. 7799D-AVR–11/10. 2010. Accessed: Feb. 12, 2023. [Online]. Available: https://ww1.microchip.com/downloads/en/DeviceDoc/doc7799.pdf

[43] “Arduino Uno SMD.” Accessed: Feb. 12, 2023. [Online]. Available: https://docs.arduino.cc/static/d2de412a57c1111cd6be956b74bc0f2b/A000066-datasheet.pdf

[44] Sensata Technologies, “D-HR Series High Insulation Resistance, High Voltage Relays-5kV, 7.5kV,10kV & 15kV,” 2020. [Online]. Available: www.cynergy3.com

[45] B. Dong, J. M. Bauchire, J. M. Pouvesle, P. Magnier, and D. Hong, “Experimental study of a DBD surface discharge for the active control of subsonic airflow,” J Phys D Appl Phys, vol. 41, no. 15, Aug. 2008, doi: 10.1088/0022-3727/41/15/155201.

[46] “DuPont TM Kapton ® is used in applications such as the solar array and for thermal management in the United States space program.”

[47] G. LaVision GmbH, “1003001_DaVis_D10.1 – Product Manual for DaVis 10.1.” LaVision GmbH, Anna-Vandenhoeck-Ring 19, D-37081 Göttingen, Mar. 2020.

Appendices

Appendix A. Davis Settings

Setting name	Setting Value
Scale Factor	12.3
Dt [μs]	7.9
Dx [px]	8
Dx [mm]	0.65
Frequency [Hz]	643
U [m/s]	82.51

Appendix B. Characteristics of Switching Driver MCU

As per the specifications given in the official Arduino® datasheet (https://www.arduino.cc/en/uploads/Tutorial/595datasheet.pdf) an Arduino UNO is able to produce clock speeds in the range of 57-100MHz. Thus, to achieve required switching frequencies of ~300Hz for up to four switches it is reasonable to conclude that in the worst case each switching operation can take up-to $57{,}000{,}000/(4 * 300) = 47{,}500$ clock cycles. Typical GPIO switching can be achieved in double digit clock cycles using the Ardiuno standard library. Therefore, even leaving a great deal of clock cycles for the Loop elements this apparatus can achieve many times faster switching than is required.

Appendix C. Apparatus Specifications

Fig 12 ID #	Explanation	Manufacturer	Part #
12.3	Laser power supply	Litron Lasers	LPU550B SN: 90290/0086
12.3	Laser head	Litron Lasers	BERNOULLI 145-15 SN LM2777
12.9	Variac	Tysun	TDGC-1 KM
12.10	High voltage transformer	Allanson	POW-R-PAK SS1235ICH
12.12 (component of array)	HV switches	Cynergy3	DAT71215F-HR (batches 0218 & 0118)

Appendix D. Test regime duty cycles

Each regime represents the duty cycles tested during one iteration of the test procedure. Each iteration includes multiple tests at varying locations, each of which generates a dataset of the average flow characteristics within a slice of the test volume.

Section	**Test Geometry**	**Purpose**	**Duty Cycle [%] of Encapsulated Electrode…**			
			1	**2**	**3**	**4**
3.3.2	1	Establish differential firing control	100	0	0	0
		Coaxial control within the plane	100	0	-	-
			0	100	-	-
3.3.3	2	Arbitrary flow within the plane of the array	50	50	-	-
			55	45	-	-
			60	40	-	-
			65	35	-	-
			70	30	-	-
			75	25	-	-
			80	20	-	-
			85	15	-	-
			90	10	-	-
			95	5	-	-
			100	0	-	-
3.3.4	3	Establishing flow out of the plane	100	100	100	100
		Measuring control of azimuthal angle	50	0	0	50
			50	5	5	50
			50	10	10	50
			50	15	15	50
			50	20	20	50
			50	25	25	50
			50	30	30	50
			50	35	35	50
			50	40	40	50

Section	Test Geometry	Purpose	Duty Cycle [%] of Encapsulated Electrode…			
			1	**2**	**3**	**4**
3.3.4	3	Displaying flow that is at an angle to the plane, the vertical axis, and all actuator geometry	50	45	45	50
			50	50	50	50
			50	50	20	50
			50	45	25	50
			50	40	30	50
			50	35	35	50
			50	50	25	45
			50	50	30	40
			50	50	35	35

Appendix E. Switch Driver Scripts

E.1

```
//two electrode configuration
gpio pin1;
gpio pin2;
int frequency = <xxx>;
int _delay = 1000/frequency;
int dutyCycle = <yyyy>;
int _delay1 = math.floor(_delay*dutyCycle/100);
int _delay2 = math.floor(_delay*(100-dutyCycle/100));
while (true){
     write(pin1, high);
     write(pin2, low);
     delay(_delay1);
     write(pin2,high);
     write(pin1, low);
     delay(_delay2);
}
```

E.2

```
//four electrode configuration
gpio pin1;
gpio pin2;
gpio pin3;
gpio pin4;
int frequency = <xxx>;
int _delay = 1000/frequency;
int dutyCycle1 = <yyyy>;
int dutyCycle2 = <zzzz>;
//adjust delays for single threaded wait times
int _delay1 = math.floor(_delay*dutyCycle1/100);
int _delay2 = math.floor(_delay*dutyCycle2/100);
int _delay3 = math.floor(_delay*(100-dutyCycle1/100));
int _delay4 = math.floor(_delay*(100-dutyCycle2/100);

if (_delay1 > _delay2){
     temp = _delay2;
     _delay2= _delay1;
     _delay1= temp;
     temp = _delay4;
     _delay3 = _delay4;
     _delay4 = temp;
}
_delay2 = _delay2-_delay1;
_delay4 = _delay4-_delay1;

while (true){
     write(pin1, high);
     write(pin2, low);
     delay(_delay1);
     write(pin3,high);
     write(pin4,low);
     delay(_delay2);
     write(pin2,high);
     write(pin1, low);
     delay(_delay3);
     write(pin4,high);
     write(pin3,low);
     delay(_delay4);
}
```